Abdominal Neoplasm: Clinical Onset in Emergency Setting

21

Barbara Sessa, Roberto Castellucci, Antonio Solazzo, Eugenio Rossi, Massimo Zeccolini, and Sandro Sironi

21.1 Introduction

The diagnosis of abdominal neoplasm in children is often delayed because the presenting symptoms tend to be nonspecific and common with the benign conditions.

The most frequent clinical presentation of paediatric abdominal neoplasm is a palpable mass, frequently in an emergency department as the first access.

When a child arrives in emergency department with a palpable abdominal mass, he requires urgent evaluation to determine if this is malignant, if it compresses vital organs or if it represents an internal haemorrhage.

B. Sessa (✉)
Department of Radiology, Papa Giovanni XXIII Hospital, Bergamo, Italy
e-mail: barbara.sessa@tiscali.it

R. Castellucci
Department of Urology, Humanitas Gavazzeni Clinic, Bergamo, Italy

A. Solazzo
Department of Radiology, Bolognini Hospital, Seriate, BG, Italy

E. Rossi • M. Zeccolini
Department of Pediatric Radiology, Pausilipon Oncologic Pediatric Hospital, Naples, Italy

S. Sironi
Department of Radiology, Papa Giovanni XXIII Hospital, Bergamo, Italy

University of Milano Bicocca, Milano, Italy

Other possible clinical presentation in emergency setting of a child with an unknown abdominal tumour is with genitourinary symptom, gastrointestinal symptom, haemorrhage, infection, anaemia, etc.

The history and physical examination, together with the age of the patient and the help of specific laboratory tests and imaging evaluations, can lead to the diagnosis. Diagnostic imaging in emergency (Miele et al. 2006; Miele and Di Giampietro 2014) plays a main role in identifying and characterizing the abdominal mass. Diagnostic techniques include X-ray studies, ultrasound, CT and MRI.

21.2 The Abdominal Physical Examination

The physical examination of the abdomen is performed with the child in supine position. It is important to note the shape of the abdomen and the position of the umbilicus. In case of a palpable mass, the following should be defined: the location, size, shape, texture, mobility and tenderness. It should be classified as solid, cystic or air filled.

A malignant mass is generally described as a non-tender, nonmobile or firm mass.

Abdominal mass is most often found in children less than 5 years of age, generally with a retroperitoneal location. The most common

© Springer International Publishing Switzerland 2016

V. Miele, M. Trinci (eds.), *Imaging Non-traumatic Abdominal Emergencies in Pediatric Patients*,
DOI 10.1007/978-3-319-41866-7_21

malignant abdominal tumour in infants is neuroblastoma followed by Wilms tumour. Other abdominal tumours in this age range include hepatoblastoma, germ cell tumours and soft tissue sarcomas (Golden and Feusner 2002).

After 10 years of age, this tumour became less frequent, but sarcomas, germ cell tumours and abdominal lymphomas increase in incidence (Marten and Kirks 1985).

21.3 Clinical Sign or Symptoms Associated

Other general signs and symptoms associated with malignant abdominal mass in a child are increased abdominal girth, pain with movement or palpation, constipation or decreased urination.

Occasionally it should be associated with weight loss, fever or decreased appetite.

Alarm symptoms, anyway common also in most benign conditions, are fever, lymphadenopathy, vomiting, pallor or localized or generalized lymphadenopathy (Fragkandrea et al. 2013).

Specific symptoms may be associated at different types of neoplasm.

Flushing, sweating and irritability may be associated to neuroblastoma because of the production of catecholamines; also an explosive and secretory diarrhoea may be caused by vasoactive intestinal polypeptides also produced by the tumour.

In Wilms tumour, there could also be possible anaemia caused by bleeding that could be profound; local stimulation of renin can result in hypertension.

Genitourinary symptoms may be associated with rhabdomyosarcoma (RMS) of the genitourinary tract; in bladder RMS, gross haematuria and decreased urinary output may be observed, with a possible progression to anuria, consisting of a genitourinary emergency.

Amenorrhoea and vaginal bleeding could be associated with ovarian germ cell tumour. Ovarian torsion or rupture of the mass could be an emergency presentation of an ovarian mass, which requires a prompt intervention.

Primary malignant tumour in children can also present as an emergency of the gastrointestinal tract; for example, acute lymphoblastic leukaemia, Burkitt lymphoma and hamartoma are often the causes of an intussusception in children more than 2 years of age.

Furthermore, many tumours may be associated with congenital anomalies.

21.4 Laboratory Testing

General laboratory studies routinely performed in emergency setting can give important information about the child's general health. They include a complete blood cell count and chemistry panel (electrolytes, liver transaminases, bilirubin, albumin, etc).

Leucocytosis can suggest a diagnosis of infection; pancytopenia can be caused by a malignant process that infiltrates the bone marrow or by an infection that stresses the marrow; anaemia can be a sign of haemorrhage into the tumour or caused by chronic disease. Thrombocytosis is often found in liver tumours. Coagulation tests are important to check the presence of disseminated intravascular coagulopathy or liver dysfunction.

A baseline urinalysis can detect the haematuria or proteinuria which can suggest a primary renal or bladder tumour. In Wilms tumour when haematuria is present, it is usually microscopic.

Other specific laboratory tests can be performed in following the steps to define, together with other elements, the specific histological characterization of the tumour (tumour markers or specific hormones produced by different tumours as neuroblastoma, phaeochromocytoma, germ cell tumours, liver tumours or teratoma).

21.5 Imaging

If an abdominal mass is suspected by a physical examination in a child who arrives in emergency department, the first imaging approach could be the ultrasound examination.

Paediatric ultrasound imaging of the abdomen is a safe, non-invasive, radiation-free, painless

test that uses sound waves, particularly valuable for evaluating abdominal, pelvic or scrotal pain in children. It is also easily available in emergency radiological setting and allows a real-time dynamic optimal visualization of the abdomen, especially in children for the characteristics of the child's body. A linear or convex probe with warmed gel may be used on the basis of the size of the baby.

It can provide detailed information about the mass location, dimensions, nature, tissue components, vascularization and relationship with the adjacent organs. With an adequate bladder distension, it is also allowed to detect the pelvic region in children with high resolution.

With the use of colour Doppler technique, it is possible to detect the mass pattern of flow.

Also contrast-enhanced ultrasound (CEUS) with intravenous injection of microbubble contrast agent could be performed in these cases, providing additional information about the enhancement of the mass and the presence of any neoplastic thrombi of the vessels involved. Despite the use of ultrasound contrast agents in children has not been officially approved since these contrast media are not licensed for paediatric use, a large survey study were carried out, which also included the use of product in intravenous route and responses suggest a favourable safety profile of this second-generation ultrasound contrast agents in children (Menichini et al. 2015).

It is already established the use of CEUS in paediatric abdominal traumatic lesions with the proliferation of a lot of studies in literature, but also in paediatric abdominal oncological emergencies, it may have a crescent role (Pinto et al. 2014, 2015; Sessa et al. 2015; Miele et al. 2015, 2016a, b, c).

When an abdominal tumour is confirmed by ultrasound is recommended a total body staging CT to better define the invasion of vessels or vital organs by the lesions and any lymph node or distant metastasis. MDCT optimization is mandatory in children, including justification for scan, patient preparation, technical and scan parameters with the low-dose CT protocols and contrast administration, with parameters of contrast material volume and flow rate depending on the age and the weight of the baby.

In some cases, it can be useful the use of MR for a more accurate detection and follow-up of oncological disease of some districts (i.e. the female pelvis, liver) or better characterization of tissue component of a detected mass; it is a free radiation exam but often requires a pharmacological sedation in children.

MR is also increasingly used in oncological disease in children, also for the introduction of fast sequences, giving very important information also with the use of new functional imaging techniques such as diffusion-weighted imaging.

When is suspected a gastrointestinal obstruction emergency presentation of the mass, it can be helpful a plain abdominal radiograph.

21.6 The Main Childhood Abdominal Malignancies

21.6.1 Neuroblastoma

It is the most common extracranial solid tumour in childhood and the most common malignancy in infants.

It accounts for about 8 % of all cancers diagnosed in children less than 15 years of age and for 15 % of all cancers in children less than 5 years of age (Matthay 1995).

Neuroblastoma arises from neural crest cells and can arise anywhere along the sympathetic chain, but 75 % of the tumours have an abdominal location and 65 % originate from the adrenal glands (Berthold et al. 1996; Calisti et al. 2012).

The clinical and prognostic behaviour of this tumour is not always predictable: it can regress spontaneously or differentiate into a benign tumour in infants, or it can have a rapidly progressive, metastatic and sometimes fatal course in children over 1 year of age. Fifteen percent of all the cancer-related deaths in children are due to neuroblastoma (Kinnier-Wilson and Draper 1974; Black 1998).

It is a solid, retroperitoneal tumour, generally fixed and unilateral, but it may cross the midline. They are lesions biologically active that produce

hormones. In 90 % of patients, the tumour excretes high levels of catecholamines and their metabolites (Graham-Pole et al. 1983; Laug et al. 1978).

21.6.1.1 Clinical Presentation

The clinical presentation is related to the production of specific hormones by the tumour, to its location and the extent of disseminated disease.

The catecholamine production can result in flushing, sweating and irritability; they can produce also vasoactive intestinal polypeptides that may cause watery, explosive, secretory diarrhoea.

Most of these tumours arise from the adrenal gland (35 % of cases), 30–35 % in the extra-adrenal retroperitoneum and 20 % in the posterior mediastinum. Less common sites are the neck (1–5 % of cases) and pelvis (2–3 %) (Morris et al. 1995).

A higher incidence of cervical and thoracic primary tumour is depicted in infants with only 25 % with an abdominal location.

Through haematogenous spread it can do metastases to the bone, bone marrow, liver and skin and in the brain and lungs in end-stage disease (Kramer et al. 2001). Only in 3% of patients there is a pulmonary involvement at the diagnosis and it is an extremely poor prognostic indicator (Kammer et al. 2001). Through lymphatic dissemination, it can affect the regional lymph nodes or nodes in other body cavities.

Abdominal distension is the most frequent presenting symptom.

Other signs and symptoms mostly associated with neuroblastoma are malaise, irritability, weight loss, shortness of breath (if it is a large abdominal tumour) and peripheral neurologic deficit (from neural foraminal invasion and nerve compression by tumour).

Other less common presentations include exophthalmos, ecchymoses, Horner's syndrome, back pain weakness, scoliosis, bladder dysfunction and palpable non-tender subcutaneous nodules.

21.6.1.2 Evaluation

Neuroblastoma, together with rhabdomyosarcoma, lymphoma, Ewing's sarcoma and leukaemia, is considered a "small, round, blue cell tumour".

An international neuroblastoma study group established the minimum criteria required to the diagnosis of neuroblastoma: (1) unequivocal pathologic diagnosis by light microscopy of tumour tissue, with or without immunohistology, or increased urine (or serum) catecholamine or metabolites and (2) bone marrow aspirate or biopsy with unequivocal tumour cells and increased urine or serum catecholamines or metabolites (Brodeur et al. 1988).

Urinary levels of homovanillic acid, vanillylmandelic acid, adrenaline, noradrenaline, dopamine and metanephrines are elevated in 90–95 % of patients with neuroblastoma (Graham-Pole et al. 1983; Laug et al. 1978).

Serum markers, although less sensitive and less specific, include ferritin, NSE and lactate dehydrogenase (LDH). The biologic factors used to stratify risks groups include (1) assessment of an oncogene called n-myc, (2) DNA ploidy and (3) specific histologic characteristics. Amplification of the proto-oncogene n-myc located on the short arm of chromosome 2 is associated with advanced stage disease and poor prognosis (Brodeur 1995; Broduer et al. 1994, 1997).

The DNA content (DNA index or DI) refers to ploidy or the chromosome complement in tumour cells. A normal chromosome number in a somatic cell is diploid (1=46 chromosomes), more is hyperdiploid, >1, and less is aneuploid, <1. A DNA index higher than 1 is associated with a favourable outcome, and an index of 1 or lower has a worse outcome (Seeger et al. 1985).

Two histological classification systems are used in the United States to stratify neuroblastic tumours into risk groups: the Pediatric Oncology Group (POG) classification and the Shimada classification (Joshi et al. 1992; Shimada et al. 1999).

The POG system is based on the degree of differentiation of the histologic elements; in particular neuroblastoma contains less than 50 % differentiated elements. It may be further subclassified as undifferentiated, poorly differentiated or differentiating (Joshi et al. 1992).

The Shimada classification is a morphologic characterization system based on the presence or absence of Schwannian stroma, the age of patient,

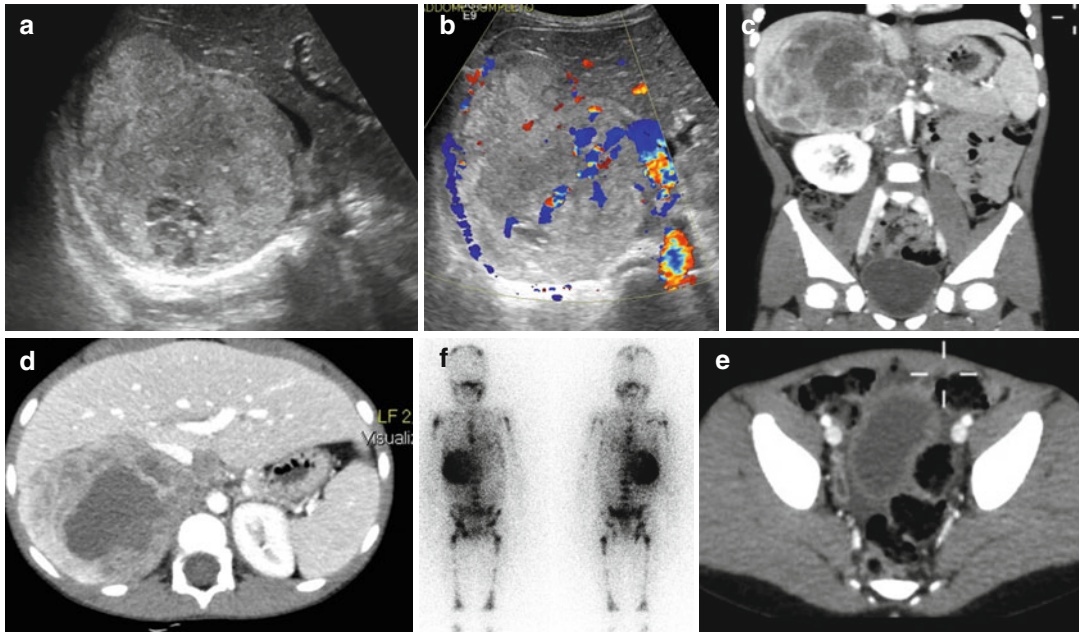

Fig. 21.1 Male, 7 years old. The child went in emergency department with a palpable mass and pain at right abdominal quadrants. Right adrenal gland neuroblastoma was discovered. US (**a**, **b**): a heterogeneously echogenic hypervascular right adrenal mass with hypoechoic area inside was depicted. CT (**c**, MPR coronal reconstruction and **d**): it shows a large and heterogeneous right adrenal mass with low-attenuation areas of necrosis or haemorrhage. Vessels were compressed but not invaded. Celiac lymph node involvement was depicted. The baby has also acute appendicitis (**e**). The 123 MIBG scintigraphy (**f**), in anterior and posterior views, shows the radiopharmaceutical uptake in primary tumours

the degree of cellular maturity and the nuclear characteristic; it is an independent prognostic indicator, either favourable or unfavourable (Shimada et al. 1999).

21.6.1.3 Imaging

Children present in emergency department with abdominal distension, constipation and abdominal pain could be generally investigated with an abdominal plain radiography and/or abdominal ultrasound.

Radiographs may show a posterior retroperitoneal, mediastinal or neck mass. Calcification is evident in at least 30 % of neuroblastoma at plain radiography (Stark et al. 1983).

Posterior mediastinal tumours may cause spreading or erosion of adjacent ribs, and both retroperitoneal and posterior mediastinal tumours may cause pedicle erosion (Miele et al. 1996). Skeletal metastases may also appear as focal lucent (occasionally sclerotic) areas (Stark et al. 1983; Miele et al. 1996; Abramson 1997).

At ultrasonography (US) neuroblastoma is generally heterogeneously echogenic (Figs. 21.1 and 21.2). It should have anechoic areas within the tumour corresponding to haemorrhage or necrosis. Calcifications are common and appear as focal echogenic areas. US may delineate the tumour from adjacent organs such as kidney, making determination of adrenal origin; when the tumour invades the kidney, this is difficult.

US and also CEUS may also evaluate the other organs such as liver, the presence of lymph nodes, the vascular invasion and so on (Stark et al. 1983; Miele et al. 1996; Abramson 1997); however these parameters are better detected by CT or MR imaging.

CT is the most commonly used imaging modality for the assessment of neuroblastoma to evaluate the extent of tumour, organ of origin, regional invasion, vascular encasement, adenopathy and calcification (Figs. 21.1 and 21.3). CT of the chest, abdomen and pelvis is the gold standard technique for all new diagnosed cases.

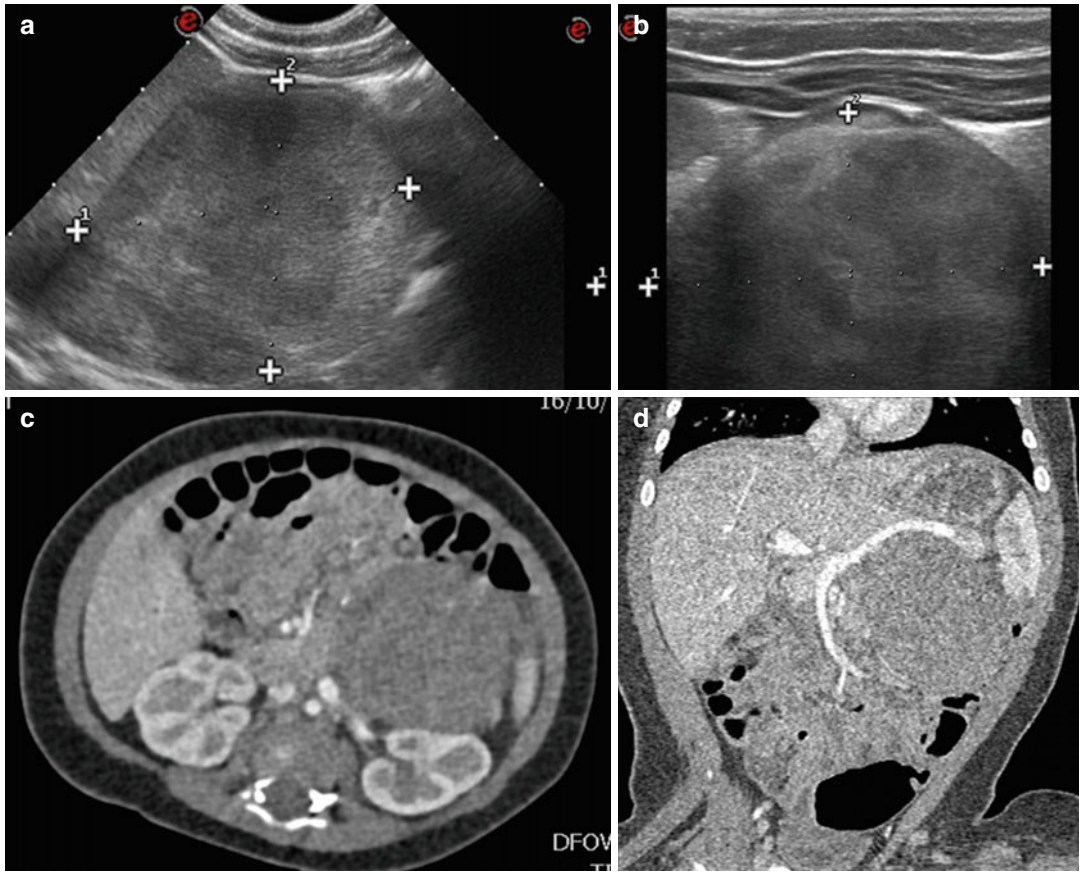

Fig. 21.2 Female, 1 year old. She presents with abdominal distension and nausea. A left adrenal gland neuroblastoma was depicted. US scans (**a**, **b**) show a quite homogeneous echogenic adrenal mass. CT (**c** and d MPR coronal reconstruction): a quite large homogeneous left adrenal mass with regular margins, not invading adjacent structures and vessels

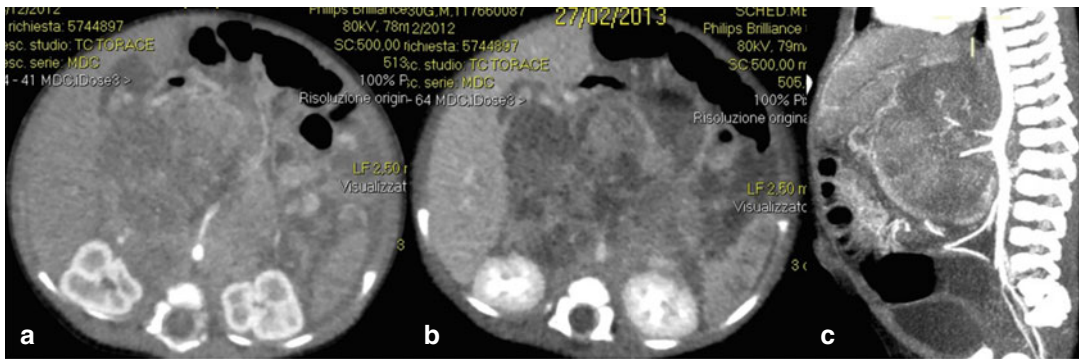

Fig. 21.3 Male, 3 years old with abdominal distension and malaise and weight loss. A retroperitoneal neuroblastoma. MDCT in arterial and venous phase axial scans (**a**, **b**) and MPR sagittal MIP reconstruction (**c**) show a retroperitoneal neuroblastoma. A heterogeneous large retroperitoneal large mass at the level of the celiac vessels was depicted. The sagittal MPR shows the encasement of the celiac tripod and the superior mesenteric artery

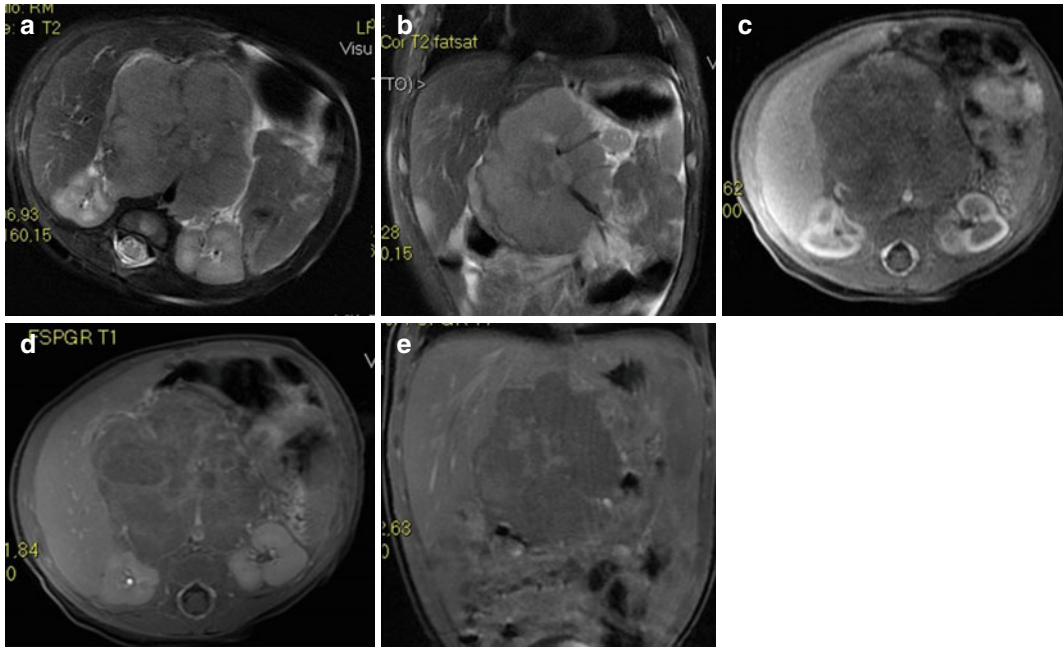

Fig. 21.4 MR exam of the retroperitoneal neuroblastoma at celiac tripod. T2w axial and coronal images (**a**, **b**). T1w axial images in arterial and venous phase and T1w coronal venous phase after Gd administration (**c**–**e**). The large retroperitoneal neuroblastoma at the level of the celiac vessels shows a relatively high signal intensity on T2-weighted images and a heterogeneous CE after Gd injection in arterial and venous phases

Abdominal and pelvic tumours are usually large and heterogeneous; 80–90 % of neuroblastomas demonstrate calcification on CT scans, and low-attenuation areas of necrosis or haemorrhage are frequently depicted (Stark et al. 1983; Miele et al. 1996; Abramson 1997). Small tumours may be homogeneous.

Vascular invasion is rare; vascular encasement and compression of the renal vessels, splenic vein, inferior vena cava, aorta, celiac artery and superior mesenteric artery may occur.

Regional invasion of psoas and paraspinal musculature may also occur, and invasion of the neural foramen into the epidural space is also frequent and better evaluated in MR imaging (Dresler et al. 1979; Aronson et al. 1995; Kenny et al. 1995).

Adenopathy of the renal hilum, porta hepatis and retroperitoneum may be seen.

Metastases at liver or lung are also depicted by CT. Liver metastases may take two forms: diffuse infiltration and focal hypoenhancing masses.

Brain metastases are unusual.

At MR imaging neuroblastoma is typically heterogeneous, variably enhancing and of relatively low signal intensity on T1-weighted images and high signal intensity on T2-weighted images (Fig. 21.4). Calcifications may be difficult to detect at MR imaging. Haemorrhagic areas may be depicted as area of high signal intensity on T1w images and cystic change may appear bright on T2w images (Dietrich et al. 1987).

MR imaging is the better modality to detect intraspinal extension of primary tumour; it should be performed at any patient with a paraspinal tumour (King et al. 1975). MR may also detect marrow disease, appearing as areas of low signal intensity on T1w images and high areas on T2w images (King et al. 1975; Siegel et al. 1986; Couanet et al. 1988).

Finally MR imaging is superior to CT in the detection of diffuse hepatic metastases in infants with stage 4S disease, as areas of high signal intensity on T2w images (Abramson 1997).

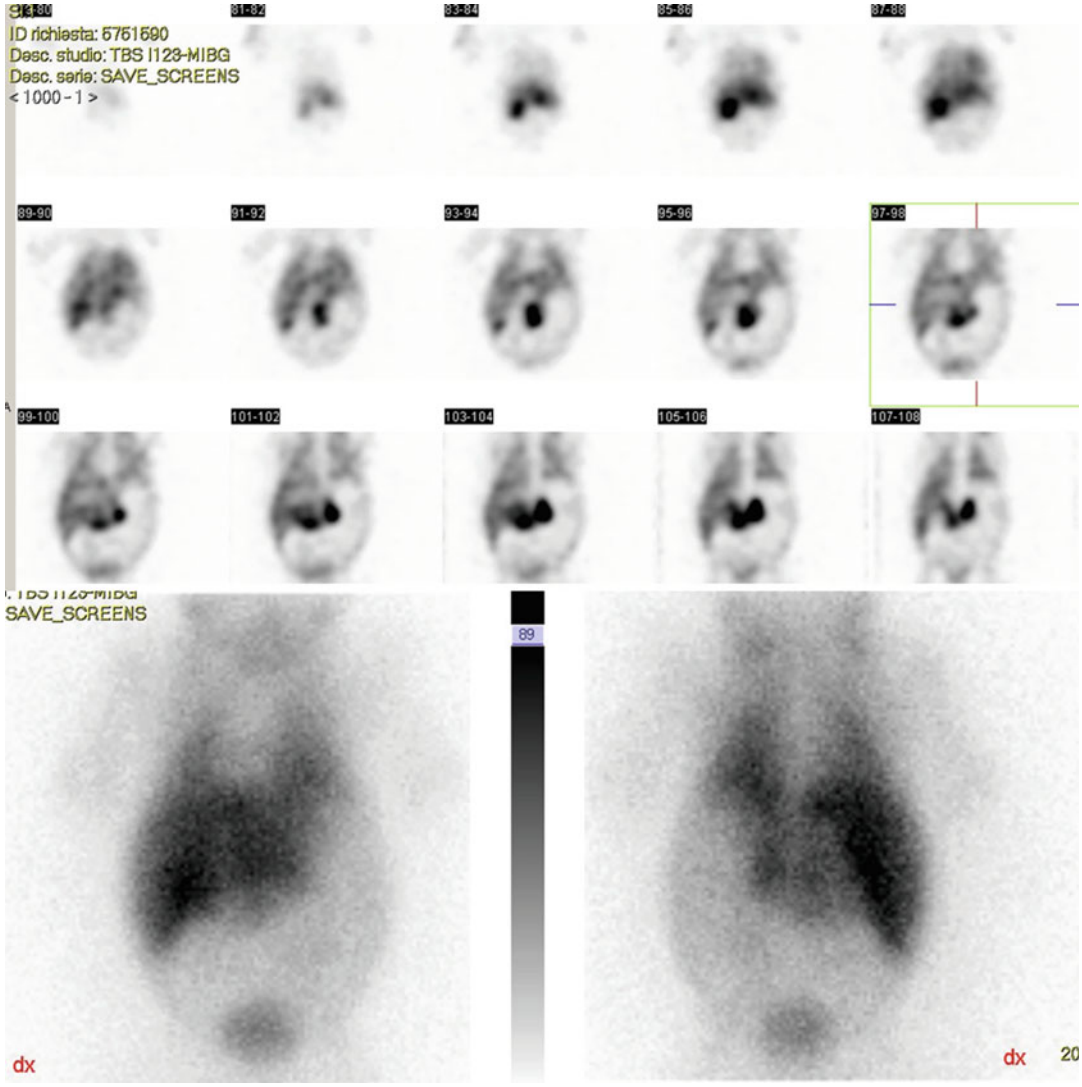

Fig. 21.5 Retroperitoneal neuroblastoma at celiac tripod. I 123 MIBG scintigraphy. The radiopharmaceutical was uptaken by the mass

Scintigraphic evaluation of neuroblastoma may be used to identificate the primary tumour and for metastatic surveillance.

For the first aim, it was performed with either a catecholamine analogue, metaiodobenzylguanidine labelled to iodine-123, referred to as MIBG (Figs. 21.1 and 21.5), or a somatostatin analogue (pentetreotide labelled to indium-11). MIBG is taken by catecholamine-producing tumours but only 70% of neuroblastomas are MIBG positive. When a tumour is evaluated by MIBG scintigraphy and is positive, it gives an excellent map of disease, but it does not allow marrow to be distinguished from cortical disease, which may be important for staging.

The 111 pentetreotide scintigraphy may also demonstrate neuroblastic tumours, but it does not appear to be superior to MIBG scintigraphy (Frappaz et al. 1997; Hattner et al. 1984; Shulkin et al. 1992; Biasotti et al. 2000; Andrich et al. 1996; Shalaby-Rana et al. 1997).

A more commonly performed scintigraphic examination is TC-99 m MDP scintigraphy which is done for evaluation of bone disease, both cortex and marrow.

TC-99 m MDP scintigraphy is initially performed on all patients with neuroblastoma to assess metastatic setting because it is more sensitive than plain radiographs in the detection of bone metastases from neuroblastoma, depicted as focal areas of an increased uptake or an increased uptake at the metaphysis (Gilday et al. 1977; Heisel et al. 1983).

21.6.1.4 Staging

Clinical staging of neuroblastoma is necessary to determine the optimal course of therapy.

The determination of the primary tumour size and the invasion of adjacent structures, the study of the liver and the lymph nodes for metastatic disease and the assessment of tumour resectability detected by CT and MRI are necessary to stage the disease.

The International Neuroblastoma Staging System (INSS) is generally used (Brouder et al. 1993) (Table 21.1).

Tumours that are grossly completely resected and have no adherent positive lymph nodes or metastases are stage 1; tumours that invade one side of the neural canal are stage 2. Tumours that extend across the midline are stage 3. When marrow involvement with tumour cells is less than 10 % of all marrow cells in the biopsy specimen, it is stage 4S; when the tumour cells are greater than 10 % of all marrow cells, the stage is 4 (Brouder et al. 1993).

Table 21.1 Neuroblastoma staging

Stage	Characteristics
Stage I	Localized tumour, complete gross total resection. Microscopic residual disease may be present
Stage IIA	Localized tumour, gross residual disease
Stage IIB	Localized tumour with ipsilateral lymph node involvement whether or not resectable
Stage III	Invasion of tumour across the midline either by direct extension or contiguous lymph node involvement
Stage IV	Disseminated disease with metastases to distant lymph nodes, bone, bone marrow, liver or other organs (except for those patients defined as IVS)
Stage IVS	Limited to age <1 year of age, localized primary (as in stages I, IIA or IIB) with metastases limited to the skin, liver or bone marrow

21.6.1.5 Prognosis and Therapy

Age and clinical stage are the two most important independent prognostic factors. Children less than 1 year of age at diagnosis have a better outcome than those diagnosed later regardless of stage disease.

Patients with localized disease also have a better prognosis. Favourable biologic characteristics include non-amplification of n-myc, a DNA index greater than 1 and a favourable histology by Shimada classification.

Management of patients with neuroblastoma is based on the risk for recurrent disease.

Stage I tumours are low risk and are treated only with surgery and observation, regardless of biologic factors.

Stage IIA-IIB tumour treatment depends on age, n-myc status and histology.

Patients with stage III tumour are treated as intermediate- or high-risk patients on the basis of age and biology.

Stage IV patients under the age of 1 year without n-myc amplification are intermediate risk, all other are high risk.

Stage 4S (special) disease infants have disseminated disease but paradoxically have a favourable prognosis with spontaneous regression. In this group histologic classification and n-myc status are fundamental for therapeutic decision-making; patients with amplification of n-myc need intensive chemotherapy treatment (Evans et al. 1996; Kushner et al. 1996; Matthay et al. 1989; Perez et al. 2000).

Adjuvant therapy is also recommended in patients with life-threatening symptoms such as vascular compromise caused by hepatomegaly, significant respiratory distress renal or bowel ischemia, obstruction of internal organs or coagulopathy (Matthay et al. 1994).

Radiation therapy should be used in the subset of patients with IVS disease that is symptomatic because of spinal cord compression or massive hepatomegaly.

Low-risk patients are treated with surgical excision and then observation.

After a gross total resection, the relapse-free survival is 90 % (Nitschke et al. 1988).

21.6.2 Wilms Tumour

Wilms tumour is the second most common abdominal tumour of childhood, is the most common renal tumour and accounts for approximately 6 % of all childhood cancers. The peak age at diagnoses is 2–3 years; it is rare in infants; a renal mass in a neonate is more likely a congenital mesoblastic nephroma (Crist and Kun 1991).

It is bilateral in 4–13 % of children (Lonergan et al. 1998).

They arise from pluripotent embryonic renal precursor cells; nephrogenic rests are metachronous disease in patients with nephrogenic rests. In only 1 % of cases, it is familial (Breslow et al. 1996; Grundy et al. 1988). It may be associated with congenital disorders and developmental abnormalities: Beckwith-Wiedemann syndrome, Sotos syndrome, Perlman syndrome and Denys-Drash syndrome. Additionally genitourinary anomalies, including hypospadias, cryptorchidism, duplicated collecting system, horseshoe kidney, cystic kidneys and renal dysplasia or aplasia, could be present.

Two loci on chromosome 11 have been implicated in the genesis of a minority of Wilms tumour: locus 11p13, known as the WT1 gene, and locus 11p15, known as WT2 gene.

The WT1 protein is mainly expressed in the development of the kidney, testis, and ovary. Constitutional deletion of this gene is often associated with WAGR syndrome, a syndrome comprising aniridia, genitourinary anomalies and mental retardation, associated with a risk of greater than 30 % for the development of Wilms tumour. WT1 deletion is also associated with sporadic aniridia and a point mutation of this gene is seen with Denys-Drash syndrome.

The other Wilms tumour gene, WT2, is associated with Beckwith-Wiedemann syndrome or hemihypertrophy (Charles et al. 1998).

Screening for Wilms tumour in patients with associated syndromes should be at 6 months of age with initial computed tomography followed by serial ultrasonography every 3 months up to 7 years of age. After the age of 7 years, screening can be discontinued because the risk of developing Wilms tumour decreases significantly (White and Grossman 1991; Beckwith 1998).

21.6.2.1 Clinical Presentation

Wilms tumour most often presents as an asymptomatic mass in the flank. It is generally large at diagnosis without significant impingement of other vital structures because of its retroperitoneal location. Approximately 25 % of patients have associated systemic symptoms or signs as malaise, pain, haematuria or hypertension. Haemorrhage is infrequent but can cause severe anaemia (Ganguly et al. 1973).

The mass is generally large, non-tender, not moving with respiration. Venous obstruction of the spermatic vein can cause varicocele. Acquired von Willebrand's disease is seen in 8 % of patients with Wilms tumour and may cause bruising or mucosae membrane bleeding.

Wilms tumour syndrome in patients with a very large tumour is a constellation of signs and symptoms as hypertension, rapid abdominal enlargement, anaemia and eggshell calcifications (Ganguly et al. 1973).

Initial laboratory evaluation includes a CBC with differential, electrolytes, creatinine, blood urea nitrogen, bilirubin, liver enzymes, serum calcium and phosphorus levels and urinalysis.

21.6.2.2 Imaging

It manifests as a solid intrarenal mass with a pseudocapsule and distortion of the renal parenchyma and collecting system; at histologic analysis, Wilms tumour is composed of variable amounts of blastema, stroma and epithelium.

The tumour typically spreads by direct extension and displaces adjacent structures but does not typically cause encasement or elevation of the aorta, findings characteristic of neuroblastoma. It may cause vascular invasion of the renal vein and inferior vena cava with occasional extension into the right atrium.

Metastases are more common in the lungs (80–85 %), liver (15 % of cases) and regional

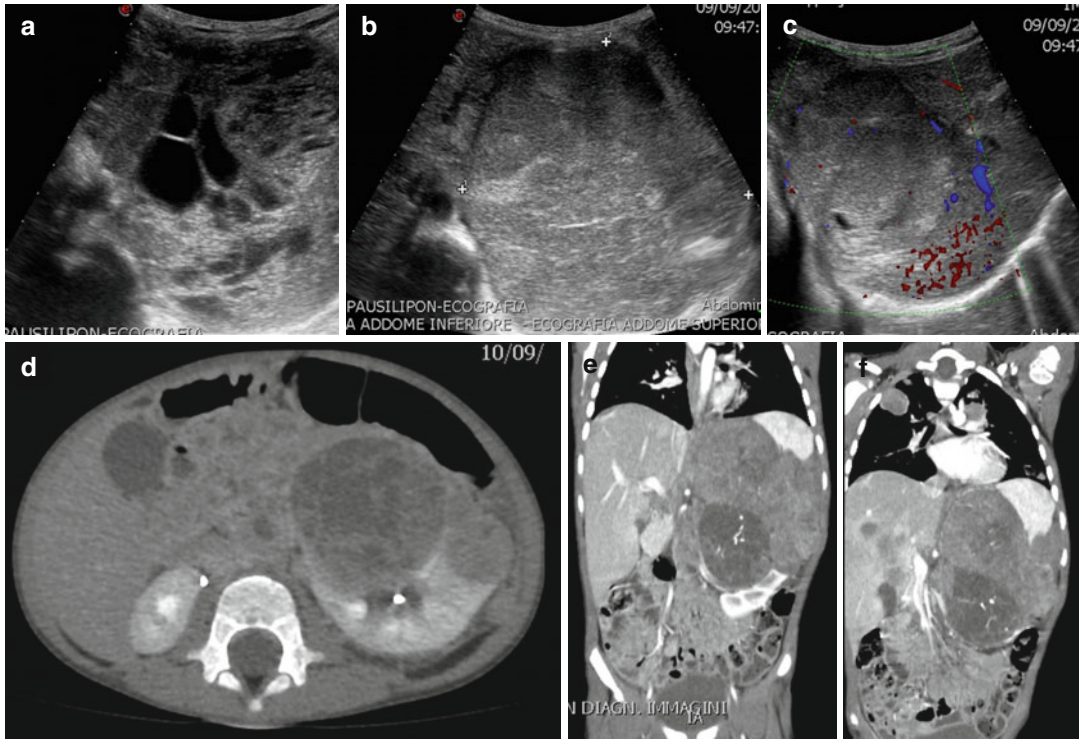

Fig. 21.6 Female, 5 years old with malaise and pain as presenting symptoms. Wilms tumour of the left kidney. US appearance (**a**–**c**): a heterogeneous echogenicity mass with necrotic areas inside. CT on axial scan (**d**) and MPR coronal reconstructions (**e**, **f**) show a solid heterogeneous intrarenal mass with necrotic areas inside and distortion of the renal parenchyma and collecting system. Also liver and lung metastases are depicted

lymph nodes, with also vascular invasion (Lonergan et al. 1998).

Ultrasound (US) is the initial imaging modality of choice in children that present in emergency department with a mass in the flank. It detects the kidney origin of the mass and quantifies the size. It most often presents as a heterogeneous echogenicity mass (Figs. 21.6 and 21.7) with hemorrhagic, fatty or necrotic areas inside and calcifications (found in only about 5–10% of Wilms tumour, unlike neuroblastoma) (Fishman et al. 1983).

US can detect also the presence and extent of tumour thrombi which could modificate the surgical approach.

CT can better depict the degree of tumour involvement of the kidney and systemic metastases (Miele et al. 1998a) (Figs. 21.6, 21.7, 21.8 and 21.9).

When a renal mass is detected by US, a chest and abdominal CT with intravenous administration of contrast material is mandatory to detect the tumour extension, presence of fat and calcifications, tumour invasion of the renal vein and inferior vena cava, contralateral synchronous tumour, associated nephrogenic rests and pulmonary, hepatic or nodal metastasis and parameters fundamental for the tumour staging.

At magnetic resonance (MR) imaging, Wilms tumour demonstrates low signal intensity on T1w and high signal intensity on T2w images. MR imaging also permits assessment of caval patency and multifocal disease. Wilms tumour is often very large at presentation and can cause severe distortion of adjacent organs, including the inferior vena cava. MR imaging has been reported to be the most sensitive modality for determination of caval patency but it requires sedation.

Wilms tumour is occasionally largely cystic; in these cases there may be difficult differential diagnosis from cystic partially differentiated

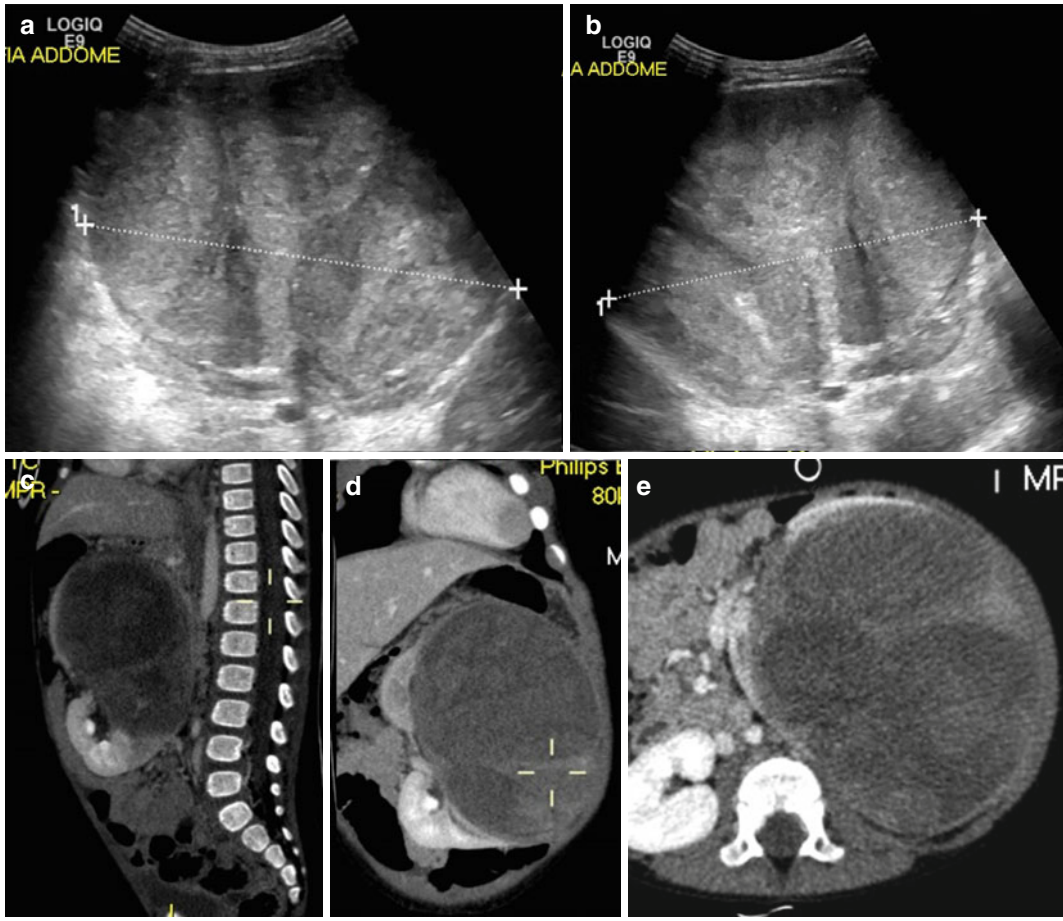

Fig. 21.7 Female, 3 years old. She presents in emergency department with a palpable mass in the left flank. US (**a**, **b**) shows a heterogeneous large predominantly hyperechoic mass with kidney origin. A MDCT (**c**, sagittal MPR reconstruction; **d**, coronal MPR reconstruction; **e**, axial scan) was then performed to better depict the degree of tumour involvement of the kidney. No metastases were depicted

nephroblastoma, a subtype of multilocular cystic nephroma treated in the next session "Neonatal abdominal masses".

21.6.2.3 Staging and Treatment

Staging and therapy for Wilms tumour depend on a timely nephrectomy with accurate surgical staging and determination of specific and biologic characteristics.

Wilms tumour staging is surgical, reported in Table 21.2 (Green et al. 1996).

Unilateral Wilms tumour is generally treated with nephrectomy followed by adjuvant chemotherapy.

Stage I and II tumours with favourable histology are usually treated post-operatively with vincristine and dactinomycin.

Patients with slightly more advanced disease also get a third drug, doxorubicin, and the length of therapy is extended. Patients with diffuse anaplasia are treated with more aggressive chemotherapy including vincristine, doxorubicin, cyclophosphamide and etoposide. In addition to surgery and chemotherapy, abdominal radiation therapy is given to all but the patients with stage I disease and those with stage II disease and favourable histology (Green et al. 1996).

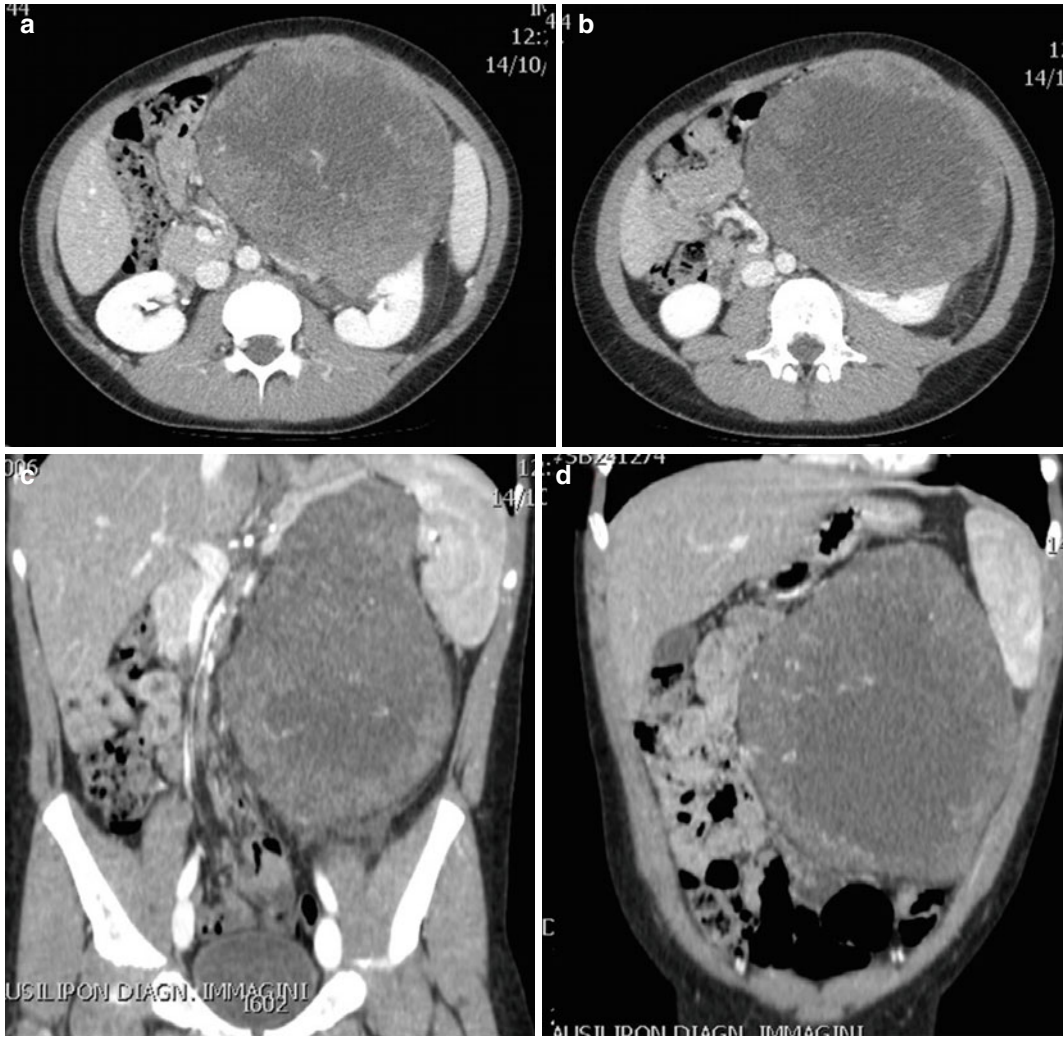

Fig. 21.8 Male, 10 years old. The child has a palpable mass in the left flank and haematuria. MDCT (**a**, **b**, axial scans; **c**, **d**, MPR coronal reconstruction) shows a large mass of the left kidney with heterogeneous contrast enhancement. A Wilms tumour at histological exam was found

Patients with pulmonary metastases may receive radiation to the lungs.

21.6.3 Hepatoblastoma

The most significant primary hepatic malignancy in neonates is hepatoblastoma, comprising approximately 1% of paediatric malignancies (Schnater et al. 2003).

The mean age at diagnoses is 1 year, with more of 80% of cases diagnosed before 3 years of age.

Hepatocellular carcinoma is much more rare and occurs in older children and adolescents, with a mean age at diagnosis of 11 years.

Hepatoblastoma may be seen in association with Beckwith-Wiedemann syndrome, with familial adenomatous polyposis (Kingston et al. 1983; Li et al. 1987) and prematurity (Feusner et al. 1997).

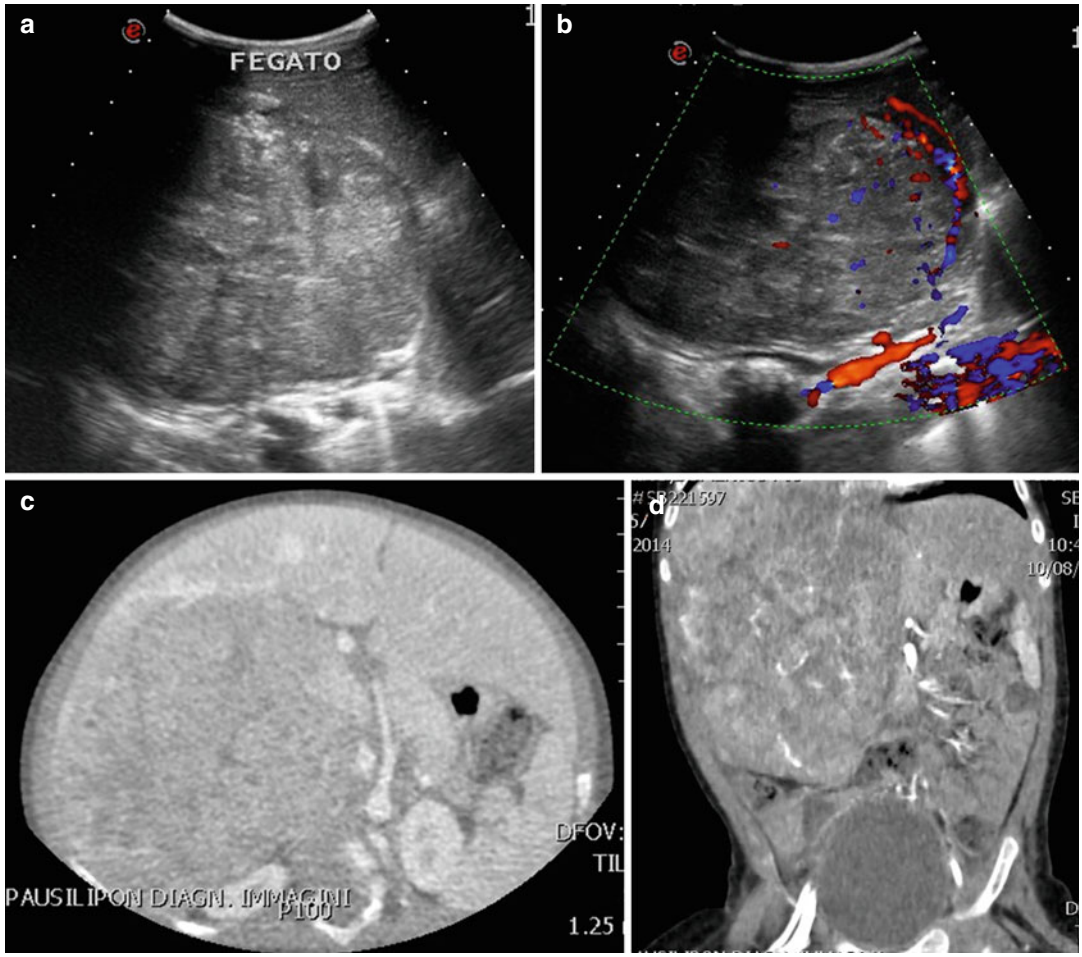

Fig. 21.9 Male, 2 years old. Child with an abdominal palpable mass and distension. US (**a**, **b**) shows a heterogeneous hyperechoic right hepatic mass, with intralesional vessel signals at colour Doppler exam (**b**). MDCT axial scan (**c**) and MPR coronal reconstruction (**d**); a very large and heterogeneous hepatic mass was depicted, with dislocation of the aorta and its branches. Hepatoblastoma was demonstrated at histological examination

The most common presentation of a child with hepatoblastoma in emergency department is an asymptomatic abdominal mass, sometimes associated with distension. Anorexia, pain or weight loss is seen in only 15–20 % of children at diagnosis. The laboratory tests in these cases include a CBC (thrombocytosis is common), urinalysis, chemistry panel including liver transaminases, electrolytes, coagulation studies (to check synthetic liver function) and hepatitis panel. Serum alpha-fetoprotein, elevated in essentially all patients with hepatoblastoma, is helpful for diagnosis and as a marker to follow during and after therapy.

Histologically the tumour presents as a large, usually solitary solid mass. It may contain fibrous bands, leading to a "spoked-wheel appearance". It can either be epithelial or mixed type and has a tendency to invade hepatic and portal veins.

21.6.3.1 Imaging

The first approach is ultrasound exam (US); on US it is detected as a solid mass with similar signal intensity compared with the surrounding liver parenchyma (Fig. 21.9). Calcifications are present in 55 % of cases and may cause acoustic shadowing. Areas of intralesional necrosis or

Table 21.2 Wilms tumour staging

Stage	Characteristics
Stage I	Tumour is limited to the kidney, renal capsule intact with or without rupture, no evidence of tumour beyond resection margin (complete resection)
Stage II	Tumour extends beyond the kidney. If there was spillage before or during surgery, it was confined to the flank, and the peritoneal surface is not involved. There is regional extension of the tumour with penetration through the capsule, invading the renal sinus or blood vessels outside the kidney. After resection, there is no evidence of tumour beyond the resection margins (complete resection)
Stage III	Gross residual tumour confined to the abdomen including any of the following: tumour penetrating the peritoneal surface, implants on the peritoneal surface, subtotal resection of tumour for any reason including infiltration into vital organs (gross or microscopic residual, or tumour spill that is beyond the flank, whether pre- or postoperative)
Stage IV	Metastases from haematogenous or lymphatic dissemination
Stage V	Bilateral renal disease, although each kidney should be staged separately (I, II or III)

tumour thrombi in the portal vein or hepatic veins may be depicted.

On unenhanced CT hepatoblastoma may have different features (Feusner et al. 1997; Miele et al. 1998b); it generally appears as a relatively well-defined, heterogeneous mass, slightly hypodense compared with liver tissue, with or without calcifications (Figs. 21.9 and 21.10). On contrast-enhanced CT, it reveals a heterogeneous enhancement and generally appears hyperdense compared with liver parenchyma in the early arterial post contrast phase and usually iso- or hypodense on delayed images. Invasion of the portal vein and thrombosis of portal or hepatic veins are well depicted by CT. Metastasis may be seen in lymph nodes and lung parenchyma, rarely in the bones and brain.

On MR hepatoblastoma is iso- or slightly hyperintense on T2w images and iso- or hypointense compared with liver parenchyma on T1w. Central necrosis may show a high T2 signal. The contrast enhancement of hepatoblastoma is similar compared with CT and quite non-specific.

Staging of hepatoblastoma depends on the extent of disease and the resectability: stage I tumours are fully resected with negative margins, stage II tumours have microscopic residual disease, stage III tumours have gross residual disease or may be only biopsied and stage IV hepatoblastoma is metastatic disease.

Therapy is surgical resection of liver disease; for large tumours or those associated with metastatic disease, chemotherapy often can finally make a total resection possible; metastatic disease without resection has a worse prognosis. If the resection is extensive, orthotopic liver transplant has been performed to cure the patient.

Chemotherapy for hepatoblastoma usually includes doxorubicin, cisplatin, vincristine, 5-fluorouracil and ifosfamide (Douglass et al. 1993).

21.6.4 Germ Cell Tumour

Paediatric germ cell tumours (GCTs) are rare tumours that include a heterogeneous group of neoplasms arising from variation of normal differentiation of germ cells; they could be benign, malignant or immature neoplasms in children and adolescent.

Eighty percent of GCTs are benign, while only 20 % are malignant representing about 2–3 % of all malignant paediatric tumours. They can develop in the gonads or in extragonadal sites (>50 %) including the retroperitoneum (Figs. 21.10, 21.11, 21.12, 21.13, 21.14, and 21.15), mediastinum or brain (Rescorla 2012).

Teratoma is the most common type with benign (mature) or immature histological features but rarely malignant. It could be classified in mature teratoma when it is composed of differentiated tissue from one or more embryonic germ layers or immature teratoma when it contains also immature epithelial or stromal tissue (Billmire 2006).

The most frequent and aggressive malignant entity in young children is yolk sac tumour (YCT) also known as endodermal sinus tumour. It can arise in all sites and can metastasize to the

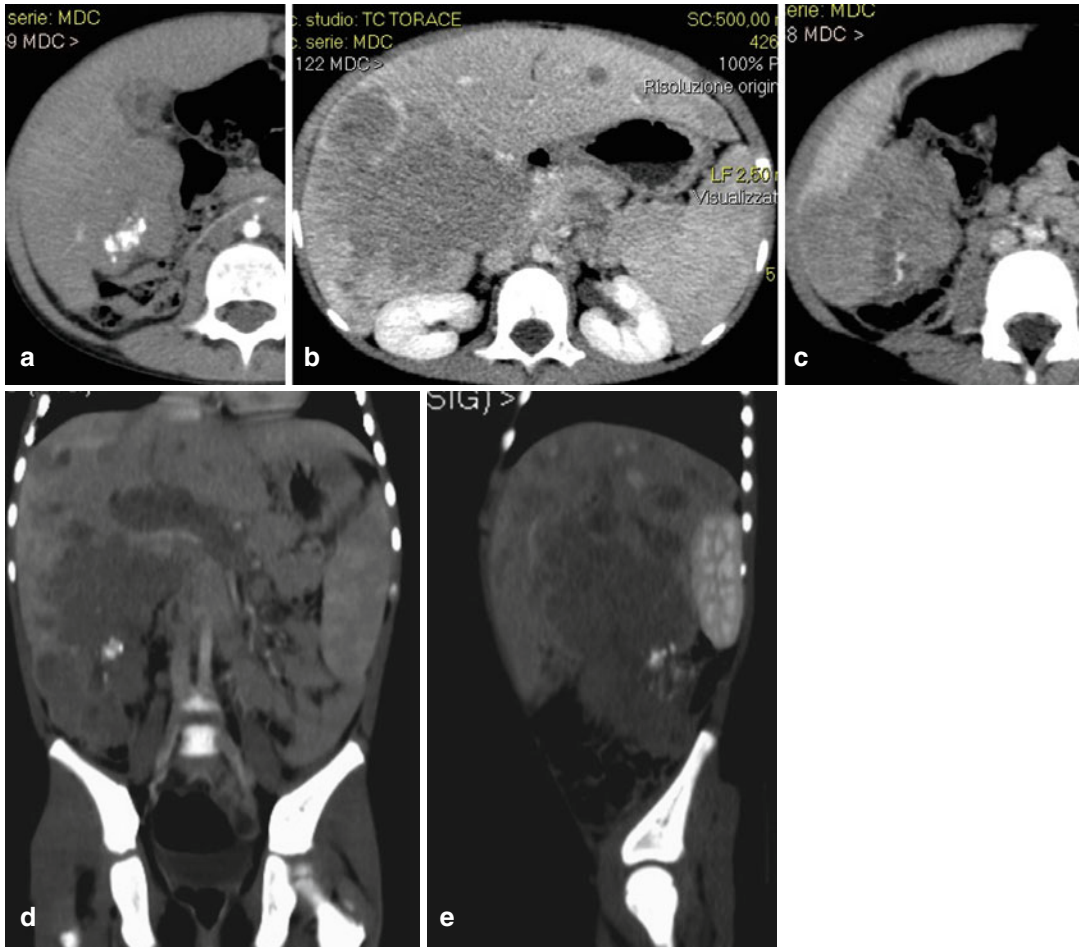

Fig. 21.10 Male, 3 years with abdominal distension and anorexia. Axial CT scan without CE (**a**) shows a hypodense hepatic area with calcifications. In MDCT scans (**b**, **c**) and MPR coronal and sagittal reconstructions (**d**, **e**), a heterogeneous hepatic lesion, relatively hypodense with inhomogeneous CE, was demonstrated. Other hepatic nodules were present. It was a hepatoblastoma

regional lymph nodes, liver, lung and brain. It is characterized by secretion of alpha-fetoprotein, a very important serum marker at diagnosis, during and after the treatment.

Other malignant histotypes are less frequent: germinomas (seminoma in males and dysgerminoma in females) are undifferentiated GCTs typical of adolescents; embryonal carcinoma and choriocarcinoma are rare differentiated forms in paediatric age which include trophoblastic cells secreting a specific serum marker, the beta subunit of human chorionic gonadotropin (beta HCG).

The most frequent localization of extragonadal GCT is the sacrococcygeal (the sacrococcygeal teratoma is treated in the session "Neonatal abdominal masses"); in the gonadal GCT, the ovarian represents about 30 % of GCTs and 70 % of all neoplastic ovarian masses (Rescorla 2008).

21.6.4.1 Ovarian GCTs

They are the most common ovarian neoplasms in children and teenagers, with a peak of incidence in early adolescence (Caruso et al. 1971).

Pathology: all the histological subtypes of GCTs may be reported in the ovary. Benign and

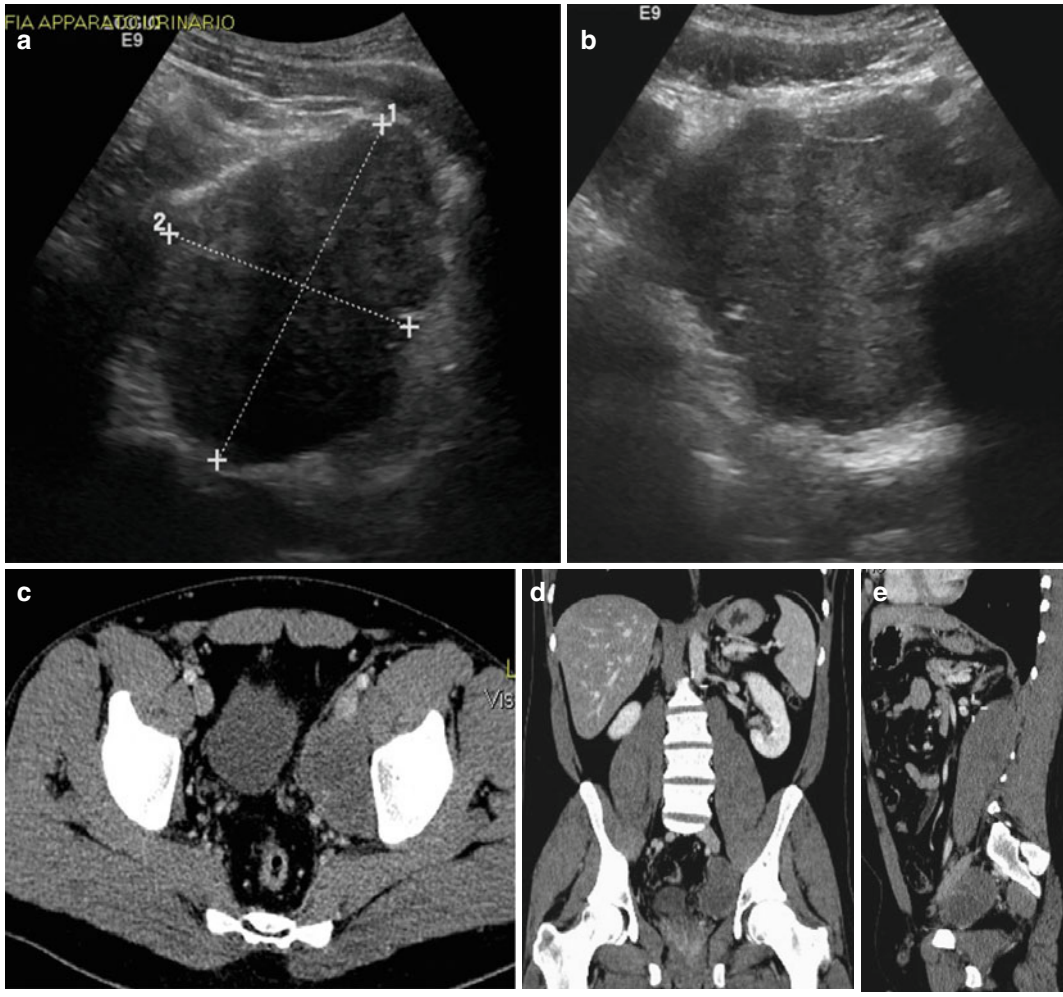

Fig. 21.11 Male, 14 years old. He presents with lower abdominal weight and pain. US (**a**, **b**) shows an inhomogeneous mass in left hemipelvic region. MDCT scan (**c**) and MPR coronal and sagittal reconstruction show the presence of solid tissue in retroperitoneal left iliac region. An extragonadic germ cell tumour was detected

immature teratomas represent about 80 % of all ovarian GCTs, bilateral in 5 % of cases. The incidence of malignant forms is reported in about 20 % and increases during adolescence (Rescorla 2012). The most common malignant entity in young people is the YSCT; dysgerminoma is the most frequent ovarian malignant GCTs in female adolescents and may be bilateral in 10 % of cases. Gonadoblastoma is rare.

The pathologic appearance of mature cystic teratomas is characteristic. In 88 % of cases, they are unilocular, filled with sebaceous material (Caruso et al. 1971). Hair follicles, skin glands, muscle and other tissues lie within the wall. There is often a raised protuberance projecting into the cyst cavity known as Rokitansky nodule. Most of the hair typically arises from this nodule. When the bone or teeth are present, they tend to be located within the protuberance (Matz 1961).

Ectodermal tissue (skin derivatives and neural tissue) is always present, mesodermal tissue (bone, cartilage, bone, fat) is seen in over 90 % of cases (Figs. 21.13, 21.14 and 21.15), and

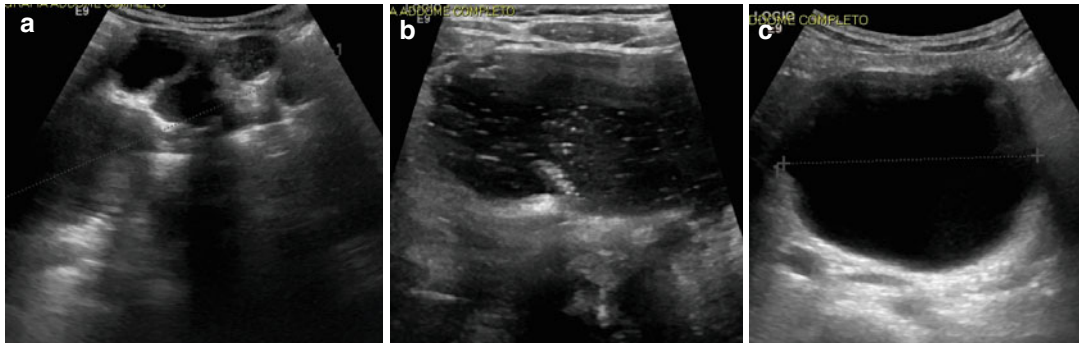

Fig. 21.12 Female, 7 years old. Presenting symptoms: constipation and abdominal distension. An US was performed as the first step, and a retroperitoneal heterogeneous mass, with a predominant sovrafluid composition, was depicted

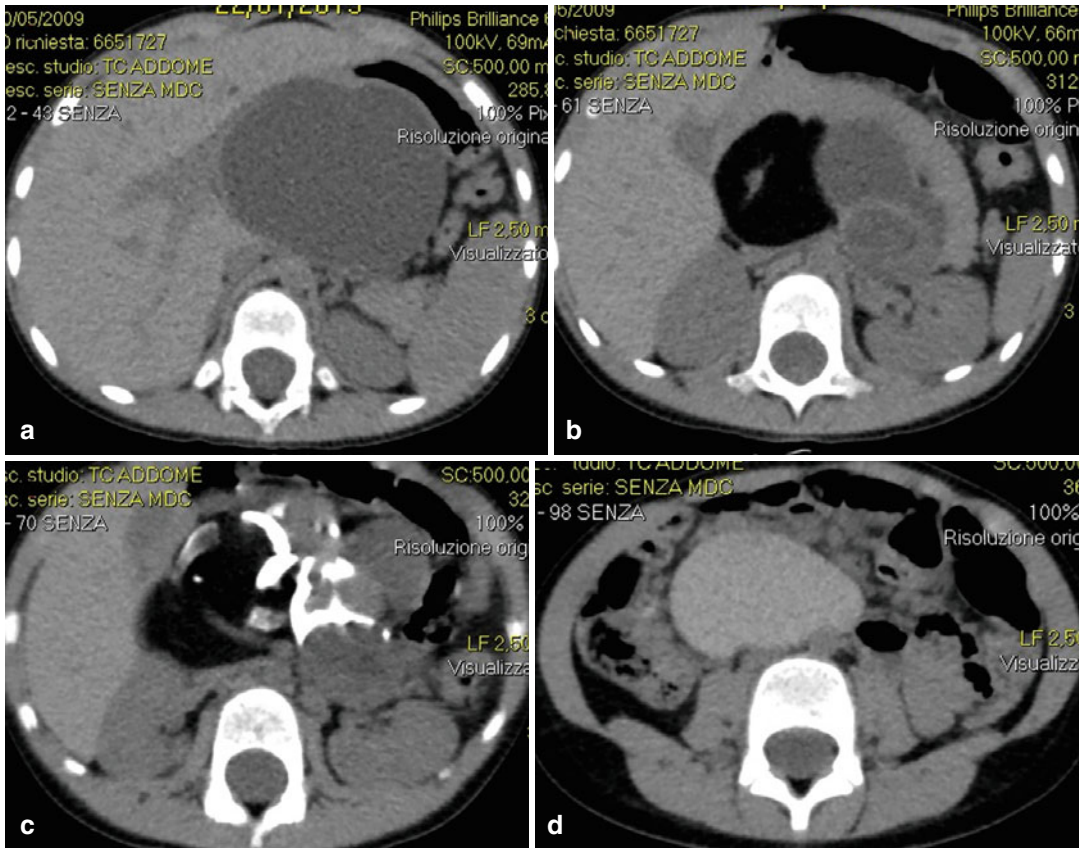

Fig. 21.13 A CT was than performed. In these unenhanced axial scans, a large retroperitoneal mass with cystic, fat, bone and sebaceous components is depicted. A retroperitoneal mature cystic teratoma was diagnosed

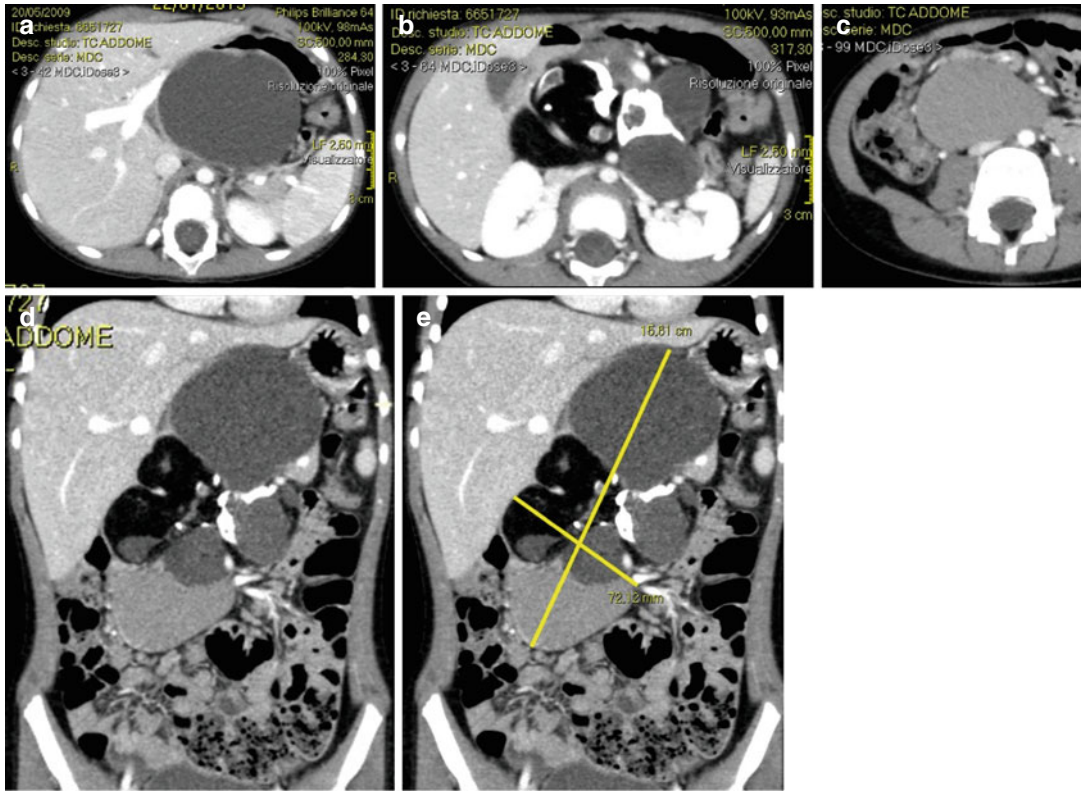

Fig. 21.14 Contrast-enhanced axial CT (**a**–**c**) and MPR coronal reconstructions (**d**, **e**) well demonstrate the large retroperitoneal mature cystic teratoma with its different components

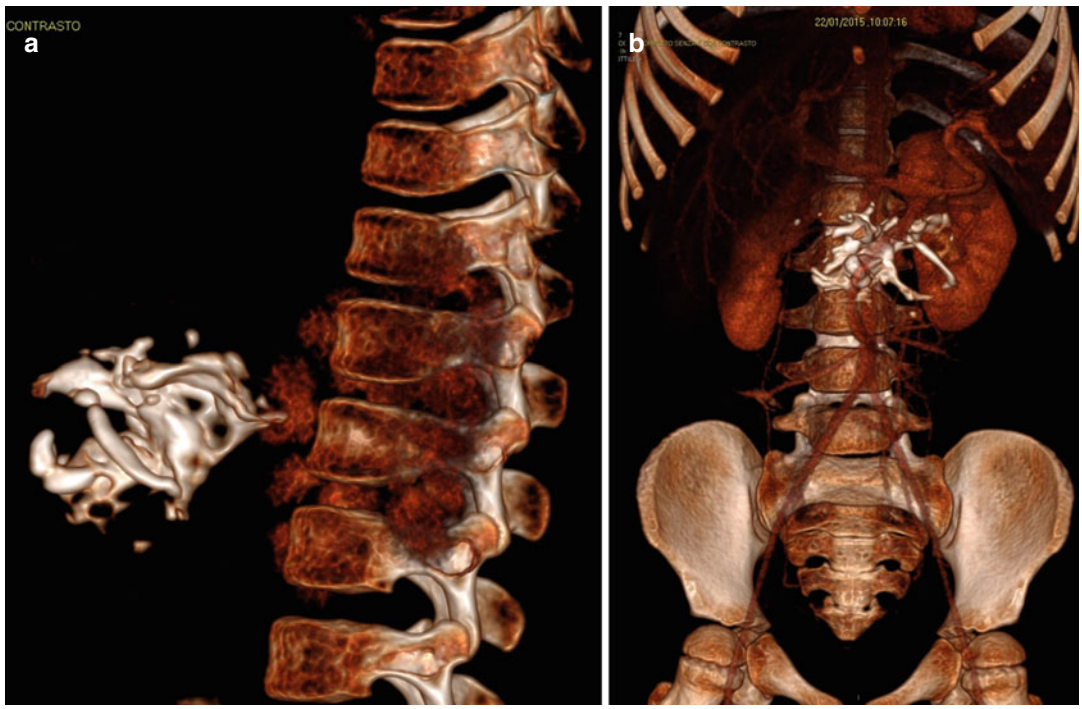

Fig. 21.15 Retroperitoneal mature cystic teratoma. VR reconstructions: the cartilaginous and bone components of the tumour seem to be rib and vertebral sketches

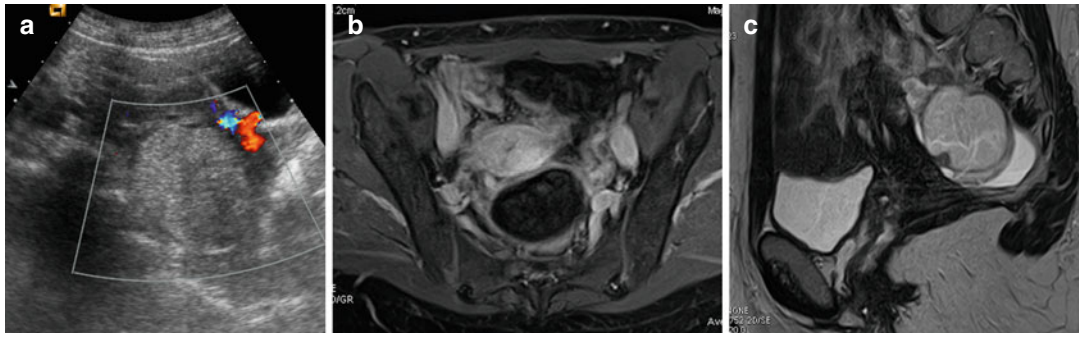

Fig. 21.16 (**a**) US scan. An oval, regular hyperechoic mass in the pelvis is detected. (**b**) Axial T1 fat sat scan after gadolinium eV. The lesion appears highly hypointense due to its fat content, with enhanced wall. In T2w sequence (**c**), a small perilesional free fluid was depicted. A dermoid ovarian cyst was diagnosed

endodermal tissue (e.g. bronchial and gastrointestinal epithelium, thyroid tissue) is seen in the majority of cases. Adipose tissue is present in 67–75 % of cases and teeth in 31 % (Caruso et al. 1971; Matz 1961).

Immature teratoma is less common, affects a younger group (usually during the first two decades of life) and has a clinically malignant behaviour. Histologically findings differ from mature teratoma in the presence of immature or embryonic tissues (Talerman 1994). They are typically larger (14–25 cm), solid or with a predominant solid composition than mature teratoma (Rescorla 2008; Talerman 1994). The cystic areas are usually filled with serous or mucinous fluid or fatty sebaceous material. A frequent perforation of the mass capsule is depicted (Talerman 1994).

Clinical presentation: abdominal pain and lower abdominal mass are the most presenting symptoms, both in malignant and in benign lesions. Constipation, amenorrhoea and vaginal bleeding are less frequent.

Beta HCG produced by choriocarcinoma can cause premature breast enlargement and pubic hair.

For the tumour with malignant components, the pattern of regional spread of malignant cells may include ascites and peritoneal metastases.

Imaging: the diagnostic workup of a young female who arrives in emergency department with a solid pelvic mass and abdominal pain usually starts with an abdominal and pelvic ultrasound (US). The US diagnosis of mature cystic teratoma may be complicated by the variety of appearances of this tumour. The tumour could appear as a cystic lesion with a very echogenic tubercle (Rokitansky nodule) into the cyst lumen or as a diffusely or partially echogenic mass with sound attenuation for the presence of sebaceous material (Fig. 21.12) and hair within the cyst or finally with multiple thin, echogenic bands (hair) in the cyst cavity. Sebum into the cyst could be hypoechoic or anechoic (Malkasian et al. 1965; Quinn et al. 1985; Patel et al. 1998). Fluid-fluid levels may be depicted (Patel et al. 1998).

More simple is the diagnosis of mature cystic teratoma by CT or MR because these modalities are more sensitive for fat. At CT fat attenuation within a cyst, with or without calcification in the wall, is suggestive for mature cystic teratoma (Figs. 21.13, 21.14, and 21.15) (Dodd and Budzik 1990; Occhipinti et al. 1993; Buy et al. 1989). At MR imaging the sebaceous component of dermoid cysts has a very high signal intensity on T1w images. The imaging appearance on T1w and T2w images may be similar to some haemorrhagic lesions (as endometrioma). Chemical shift sequences, gradient echo imaging with an echo time in which the water and fat are in opposite phase and sequences with frequency-selective for saturation help to detect fat in the lesion, distinguishing dermoid cyst and mature cystic teratoma from haemorrhagic lesions (Togashi et al. 1987; Guinet et al. 1993; Imaoka et al. 1993) (Figs. 21.16 and 21.17).

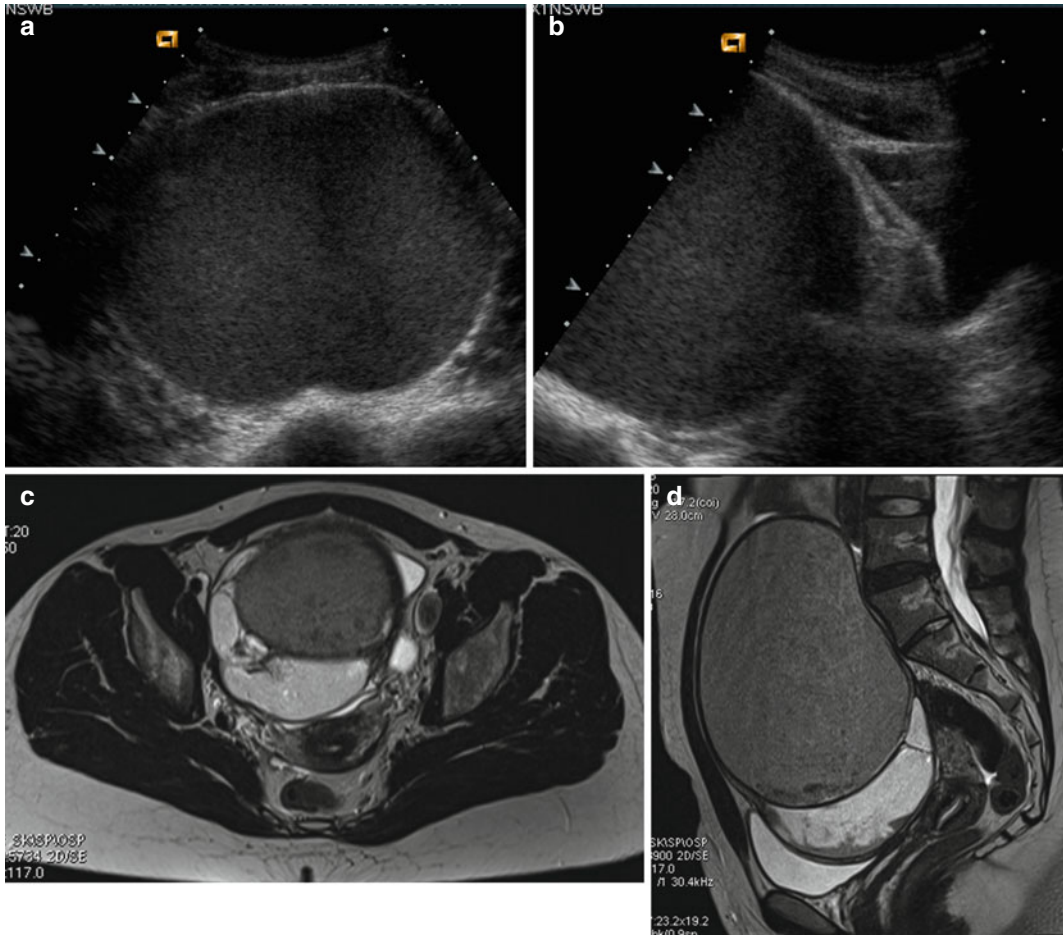

Fig. 21.17 Female, 16 years old. (**a**, **b**) Abdominal sonography: (**a**) axial scan, (**b**) longitudinal scan: huge fluid corpuscular mass completely filling the pelvic space. Bladder displaced inferiorly. (**c**, **d**) MRI, (**c**) axial and (**d**) sagittal T2w sequences confirm the ovarian neoplasm, which includes liquid and fat tissue. Mature ovarian teratoma

Mature cystic teratoma can be associated with complications from rupture (Miele et al. 2002), malignant degeneration or (most commonly) torsion in the larger mass. Findings suggestive for torsion are deviation of the uterus to the twisted side, engorged blood vessels on the twisted side, high signal intensity of the mass on T1w sequences, low signal intensity torsion knot and thick blood vessels around the lesion with complete absence of enhancement (Kimura et al. 1994).

Also immature teratomas are non-specific US appearance (Sutton et al. 1992). They are typically heterogeneous masses, with a predominant solid composition, generally with scattered calcifications. Small fat foci may be difficult to recognize. At CT and MR imaging, these tumours have a characteristic appearance: a large, irregular mainly solid mass with calcifications, small foci of fat and often hemorrhagic areas (Figs. 21.18 and 21.19) (Brammer et al. 1990; Outwater and Dunton 1995).

Laboratory tests: evaluation of serum markers may address the nature of the tumour; alpha-fetoprotein or beta HCG means the presence of malignancy (the first is raised in over 90 % of the malignant tumour, while beta HCG in 30 % of cases). Other markers as LDH and NSE or those typical for epithelial tumours (CEA, CA 125)

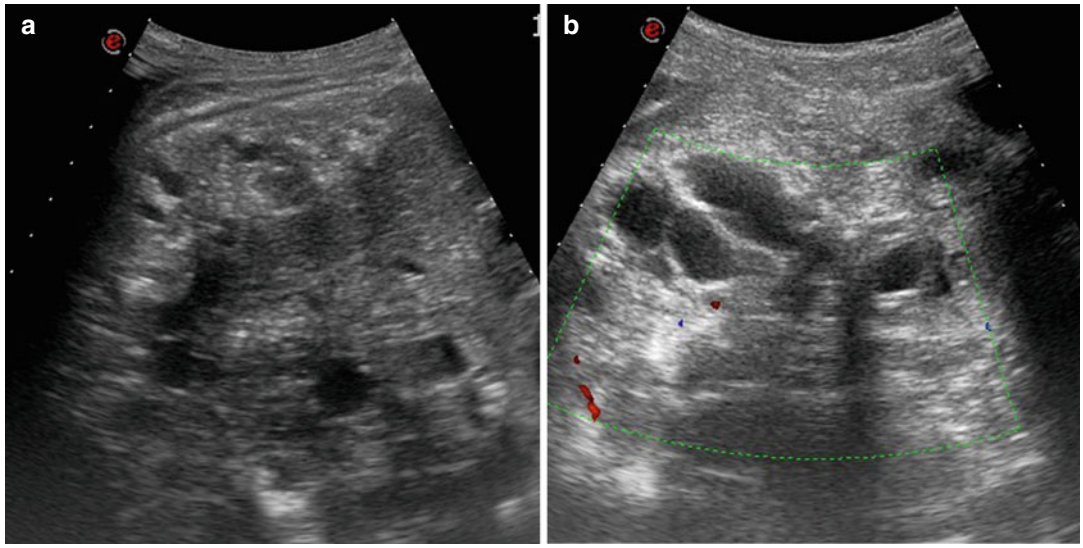

Fig. 21.18 Ovarian immature teratoma. Abdominal ultrasound. (**a**, **b**) The complex mass completely fills the pelvic space

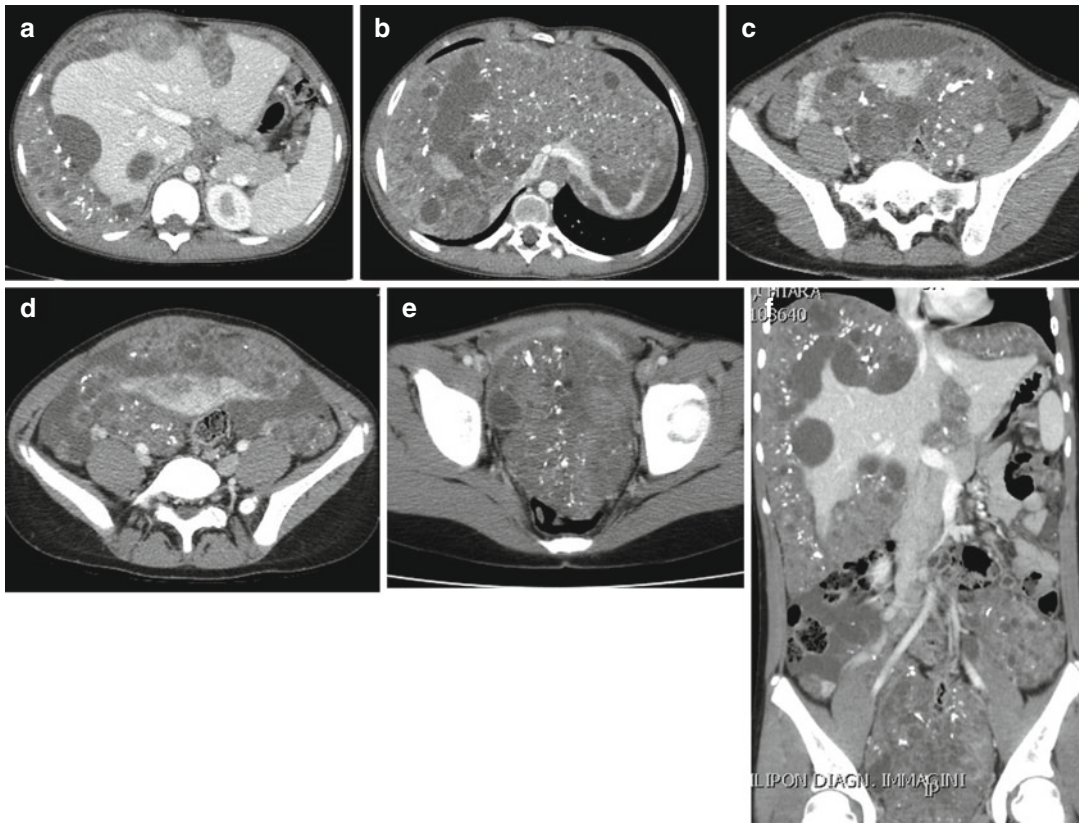

Fig. 21.19 Same patient of Fig. 21.17. CT (**a**–**e**). Bulky pelvic mass, with numerous internal calcifications. Presence of metastases to the liver, root of the mesentery, peritoneum and omentum. Ovarian immature teratoma with multiple metastases

may be elevated in patients with mixed tumours (Von Allmend 2005).

Treatment: ovariectomy and ovarosalpingectomy are the treatment of choice in malignant GCTs. However, since malignant GCTs are very chemosensitive, primary excision should be attempted only when it represents a complete but non-mutilating procedure. Generally the mass becomes surgically resectable after chemotherapy. So that this operation is not demolitive (Rescorla 2012; Billmire 2006).

The surgical technique should include well-defined intraoperative staging procedure (Rescorla 2012; Billmire 2006; Von Allmend 2005):

1. Inspection and palpation of the contralateral ovary with a biopsy of suspected areas
2. Collection of peritoneal fluid for cytology
3. Intact removal of the ovary without violation of the tumour capsule. Sparing the fallopian tube only if not adherent
4. Examination of the omentum, the peritoneal surface and the liver with removal of any abnormal areas
5. Examination of iliac and aorto-caval nodes with biopsy of any abnormal nodes

If imaging exams show involvement of neighbouring organs (i.e. the bladder, uterus and vagina) or in case of bilateral malignant GCTs, a tumour biopsy is the best option.

In case of bilateral tumours, most authors recommended to attempt ovarian preservation if possible on chemotherapy which has been proven not effective (Billmire et al. 2004).

Staging: there are two main staging systems for paediatric ovarian malignant tumours, the staging system suggested by the Children's Oncology Group (COG) and the International Federation of Gynecology and Obstetrics (FIGO) staging system. Both of them are based on the results of the imaging investigations and on the findings of the first surgical approach (Outwater and Dunton 1995; Von Allmend 2005). COG staging system is reported in Table 21.3 (Billmire et al. 2004).

Treatment of benign and immature GC: they are generally well-defined masses with larger cystic components as compared with malignant forms and do not show elevated levels of alpha FP or beta HCG.

Table 21.3 COG staging system for ovarian MGCTs

Stage	Characteristics
Stage I	Disease limited to the ovary and completely excised; negative peritoneal washing. No clinical, surgical or histological evidence of disease extending beyond the ovary and tumoural markers and/or hormonal levels in range after surgery
Stage II	Microscopic residuals, spillage or nodes affected by disease (<2 cm); negative peritoneal washing. Tumoural markers positive or negative
Stage III	Macroscopic residuals or initial biopsy only; local invasion (omentum, bowel, bladder); positive peritoneal washing; nodes affected (>2 cm). Tumoural markers positive or negative
Stage IV	Distant metastases. Negative or positive markers
Hidden disease	Stage I but tumoural markers persistently out of normal range after a complete surgery

In the first months of life, most ovarian lesions are benign and often detected an antenatal ultrasound (Bagolan et al. 1992). Most of them are observed for some months after birth until the spontaneous regression. If the lesions are very huge (more than 5 cm in size) or symptomatic, a more aggressive therapeutic approach is recommended.

The only effective therapy is the complete removal (Templeman and Fallat 2005); the procedure often requires the ovariectomy, or in selected cases with small tumours, the enucleation of the lesion can be possible. Since most GCTs are mixed tumours with mature and immature elements inside, it is sometimes impossible to know whether the lesion is malignant or not before surgery; so that intraoperative staging procedures are recommended.

Chemotherapy may be suggested only if there is the suspect of malignant transformation (Green 2008).

Ovarian torsion of an ovarian mass, often of a benign mass, may present as an acute abdomen which requires an emergent procedure usually with a laparoscopic approach

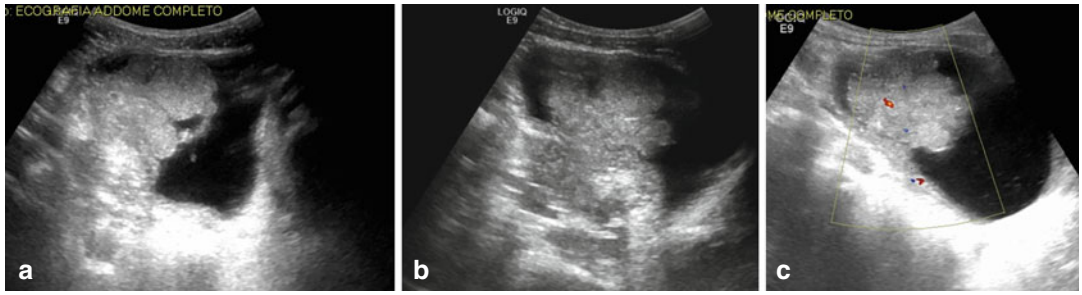

Fig. 21.20 Female, 10 years old. She reports decrease urinary output. US images show a vegetant polylobulate mass in the bladder. Bladder rhabdomyosarcoma

(Di Giacomo et al. 2015). Immediate ovariectomy is necessary only in the setting of an ischemic or necrotic ovary.

21.6.5 Rhabdomyosarcoma

Rhabdomyosarcoma (RMS) is one of the most common malignant solid tumours of childhood, after neoplasms of the central nervous system, neuroblastoma and Wilms tumours (Agrons et al. 1997). The genitourinary tract is the second most common site of RMS, behind the head and neck.

The median age at presentation is 7 years, with variability in presentation secondary to the different sites of origin within the genitourinary tract (the bladder, prostate, testes, paratesticular region, penis, vagina, perineum and uterus). Bladder RMS may cause hydroureteronephrosis, gross haematuria and decreased urinary output with a rapid progression to anuria.

Most of patients with RMS have metastasis at the time of diagnoses at lungs, cortical bone and lymph nodes.

Sonography of the genitourinary system and the other abdominal organs can be helpful to detect the site of origin and the invasion of adjacent or remote structures. The sonographic, CT and MRI appearance of the tumour is variable, generally is solid mass, with haemorrhage or necrotic areas inside (Fig. 21.20, 21.21 and 21.22).

Treatment is surgical excision, often after adjuvant chemotherapy to reduce primary tumour size (Agrons et al. 1997; Maurer et al. 1988).

21.7 Neonatal Abdominal Masses (Younger than 1 Year of Age)

21.7.1 Congenital Mesoblastic Nephroma

Congenital mesoblastic nephroma (CMN) is the most common abdominal neoplasm in the neonate, typically presenting in children at a mean of 3 months as a palpable abdominal mass (Pinto and Guinard 1995; Marsden and Lawler 1983). CMN is generally a benign lesion with some malignant potential; so nephrectomy and complete resection are necessary.

Sonographic findings of this tumour include a large solid renal mass with heterogeneous or low echogenicity (Fig. 21.24), with internal flow at colour Doppler exam. A central hypoechoic area of necrosis can be depicted. The mass may extend beyond the capsule but does not typically involve the renal vein (Riccabona 2003).

The following exam with CT or MR is mandatory when this renal mass was found in ultrasound exam (Fig. 21.23) to exclude metastasis, because they may rarely occur in the case of cellular type pathology.

CMN can have a similar appearance to Wilms tumour, but Wilms tumour is statistically less frequent in neonates.

21.7.2 Haemangioendothelioma

Hepatic haemangioendothelioma is the most commonly diagnosed symptomatic tumour

Fig. 21.21 MDCT (**a**, **b**, coronal and sagittal MPR reconstructions; **c**, axial scan) detects the polylobulate heterogeneous mass inside the bladder with necrotic areas inside. A diagnosis of bladder rhabdomyosarcoma was then demonstrated

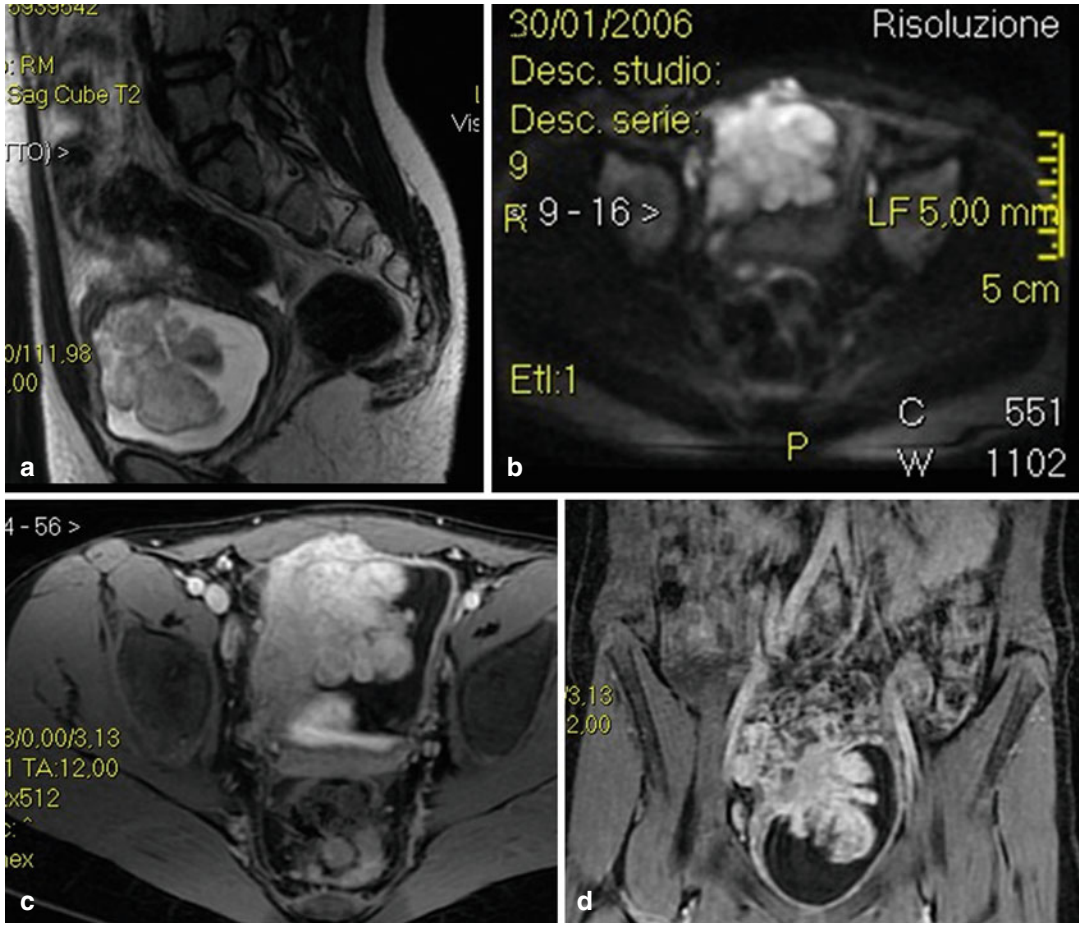

Fig. 21.22 Bladder rhabdomyosarcoma on MR images. Sagittal T2w scan (**a**) shows a isointense mass protruding into the bladder lumen; axial DWI image with b value of 600 (**b**) shows a restricted diffusion of the mass which appears bright on diffusion-weighted images. Axial and coronal contrast-enhanced T1w images (**c**, **d**) demonstrate an intense and inhomogeneous enhancement after gadolinium eV injection

in infants under 6 months of age (Selby et al. 1994; Roos et al. 2003) and represents approximately 12 % of all paediatric hepatic neoplasm. The typical presentation is a palpable right-upper quadrant mass; many infants also have cutaneous haemangiomas, leading to investigation of non-palpable liver lesions. It represents a spectrum of disease from asymptomatic mass to major arteriovenous shunting, which may lead to congestive heart failure. The Kasabach-Merritt phenomenon, which may be associated with this tumour, is the combination of thrombocytopenia, consumptive coagulopathy and haemolytic anaemia.

On US exam haemangioendothelioma typically appears as complex solid hepatic lesions with a heterogeneous echotexture, but predominantly hypoechoic (Roos et al. 2003). Doppler colour flow may be marked, depending on the amount of AV shunting (Fig. 21.24). During involution the mass can increase in echogenicity as it decreases in size. Haemoperitoneum may be present. If multiple haemangioendotheliomas are present in the liver, the disease has an unfavourable prognosis.

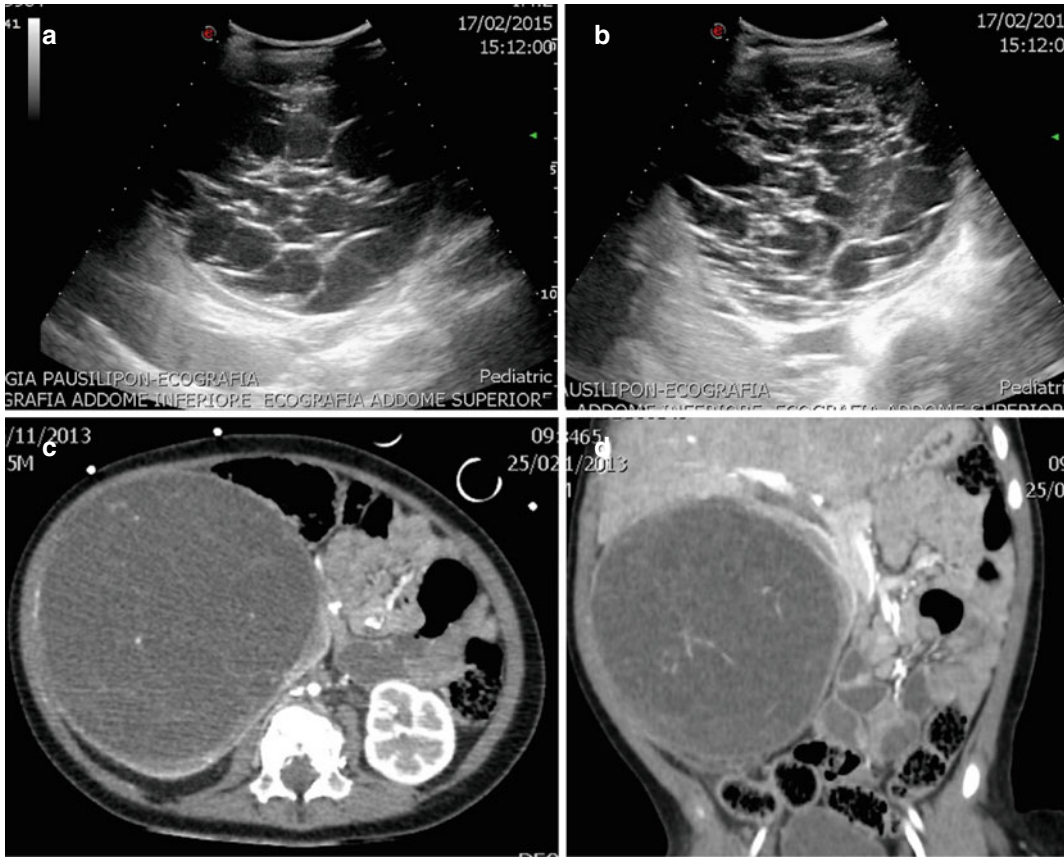

Fig. 21.23 Male, 2 years old, arrives in emergency department with a palpable mass in the right abdomen. US images (**a**, **b**): a pluriconcamerate cystic mass with right renal origin is depicted. CT scans (**c**) and MPR coronal reconstruction (**d**) show a low-attenuation cystic right renal mass with thick septations. A right renal cystic nephroblastoma was discovered

Spontaneous regression is common in patients who have a single hepatic haemangioendothelioma (Selby et al. 1994).

Various therapeutic approaches could be considered: steroids, interferon and chemotherapy; embolization and surgery are reserved for patients who have severe complications.

21.7.3 Sacrococcygeal Teratoma

Sacrococcygeal teratoma (ST) is often diagnosed prenatally because of the typical exophytic component protruding from the foetal buttock; it has a female predilection of at least 3:1 (Pantoja et al. 1976).

STs are classified by the presence or absence of internal (presacral) or external components. Serum alpha-fetoprotein levels are typically elevated with ST.

On US, CT and MR exams, ST shows variable patterns of solid and cystic areas, typically with foci of calcification and fat, and portions of cystic or necrotic areas (Figs. 21.25 and 21.26). The imaging appearance of ST cannot definitively be used to predict histology; however generally benign tumours are more likely to be cystic and malignant tumours are more likely to be solid (Keslar et al. 1994; Miele et al. 1999).

Surgical excision is the recommended treatment, with the addition of chemotherapy when malignancy is established.

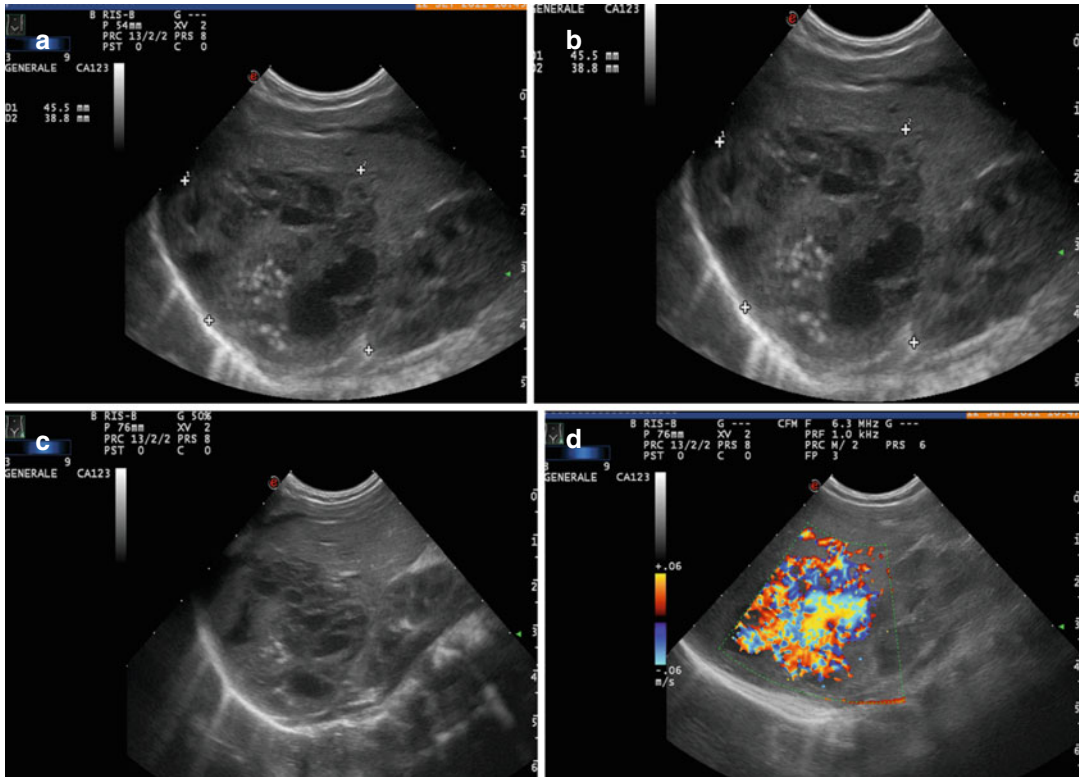

Fig. 21.24 Male, 8-day years old. He arrives with a palpable right-upper quadrant mass and a prenatal diagnoses of adrenal mass. The US images show a solid hepatic lesion with a heterogeneous echotexture, but predominantly hypoechoic. Doppler colour flow (**d**) is marked for the presence of multiple AV shuntings

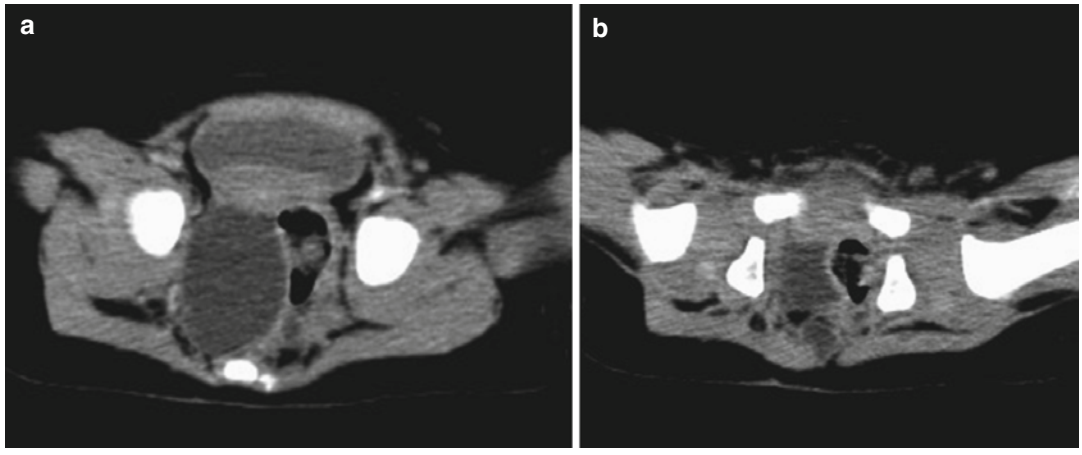

Fig. 21.25 Female, 11-month years old. CT images show a predominantly cystic sacrococcygeal mass. A sacrococcygeal teratoma was then diagnosed

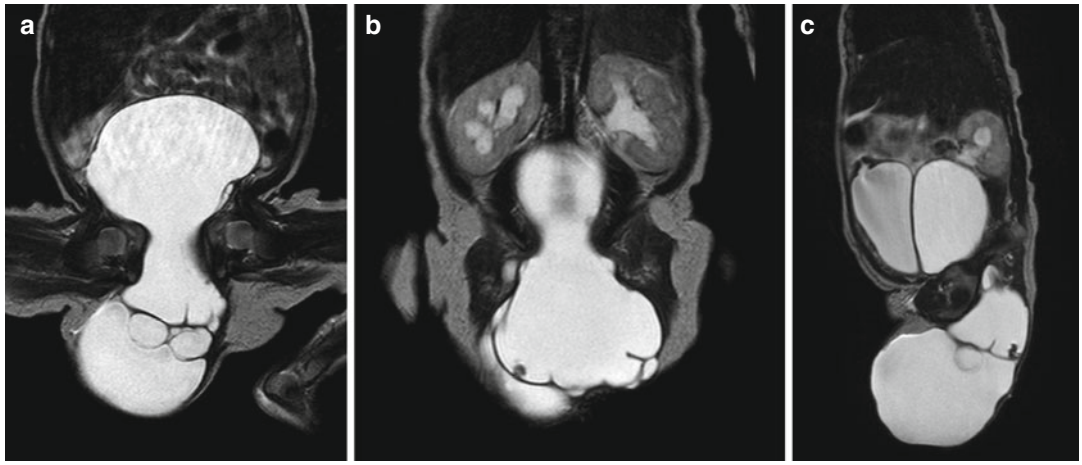

Fig. 21.26 Female. 1 year old. T2w coronal (**a**, **b**) and sagittal (**c**) images show a very large, pluriconcamerate, cystic mass with sacrococcygeal origin, extended to the mesogastrium. A sacrococcygeal teratoma was demonstrated

References

Abramson SJ (1997) Adrenal neoplasms in children. Radiol Clin North Am 35:1415–1453

Agrons GA, Wagner BJ, Lonergan GJ et al (1997) Genitourinary rhabdomyosarcoma in children: radiologic-pathologic correlation. Radiographics 17:919–937

Andrich MP, Shalaby-Rana E, Movassaghi N, Majd M (1996) The role of 131 iodine-metaiodobenzylguanidine scanning in the correlative imaging of patients with neuroblastoma. Pediatrics 97:246–250

Aronson MR, Smoker WR, Oetting GM (1995) Hemorrhagic intracranial parenchymal metastases from primary retroperitoneal neuroblastoma. Pediatr Radiol 25:284–285

Bagolan P, Rivosecchi M et al (1992) Prenatal diagnosis and clinical outcome of ovarian cysts. J Pediatr Surg 27:879–881

Beckwith JB (1998) Children at increased risk for Wilms tumor: monitoring issues. J Pediatr 132:377–379

Berthold F, Brandies WE, Lampert F (1996) Neuroblastoma: diagnostic advances and therapeutic results in 370 patients. Monogr Paediatr 18:206–223

Biasotti S, Garaventa A, Villavecchia GP, Cabria M, Nantron M, De Bernardi B (2000) False-negative metaiodobenzylguanidine scintigraphy at diagnosis of neuroblastoma. Med Pediatr Oncol 35:153–155

Billmire DF (2006) Malignant germ cell tumors in childhood. Semin Pediatr Surg 15:30–36

Billmire D, Vinocur C, Rescorla F et al (2004) Children's Oncology Group (COG) Outcome and staging evaluation in malignant germ cell tumors of the ovary in children and adolescents: An intergroup study. J Pediatr Surg 39:424–429

Black CT (1998) Neuroblastoma. In: Andrassy R (ed) Pediatric surgical oncology. WB Saunders, Philadelphia, pp 175–211

Brammer HM III, Buck JL, Haye WS et al (1990) From the archives of the AFIP. Malignant germ cell tumors of the ovary: radiologic-pathologic correlation. RadioGraphics 10:715–724

Breslow NE, Olson J, Moksness J (1996) Familial Wilms' tumor: a descriptive study. Med Pediatr Oncol 27:398–403

Brodeur GM (1995) Molecular basis for heterogeneity in human neuroblastomas. Eur J Cancer 31A:505–510

Brodeur GM, Seeger RC, Barrett A (1988) International criteria for diagnosis, staging and response to treatment in patients with neuroblastoma. J Clin Oncol 6:1874–1881

Broduer GM, Seeger RC, Schwab M et al (1994) Amplification of N-myc in untreated human neuroblastomas correlates with advanced disease stage. Science 224:1121–1124

Broduer GM, Maris JM, Yamashiro DJ et al (1997) Biology and genetics of human neuroblastomas. J Pediatr Hematol Oncol 19:93–101

Brouder GM, Pritchard J, Berthold F et al (1993) Revisions in the international criteria for neuroblastoma diagnosis, staging and response to treatment. J Clin Oncol 11:1466–1477

Buy JN, Ghossain MA, Moss AA et al (1989) Cystic teratoma of the ovary: CT detection. Radiology 171:697–701

Calisti A, Oriolo L, Molle P, Miele V, Spagnol L (2012) Neonatal adrenal masses: do we have reliable criteria for differential diagnosis and expectant management? Minerva Pediatr 64:313–318

Caruso PA, Marsh MR et al (1971) An intense clinicopathological study of 305 teratomas of the ovary. Cancer 27:343–348

Charles AK, Vujanic GM, Berry PJ (1998) Renal tumours of childhood. Histopathology 32:293–309
Couanet D, Geoffray A, Hartmann O, Leclere JG, Lumbroso JD (1988) Bone marrow metastases in children's neuroblastoma studied by magnetic resonance imaging. Prog Clin Biol Res 271:547–555
Crist WM, Kun LE (1991) Common solid tumors of childhood. N Engl J Med 324:461–471
Di Giacomo V, Trinci M, Van der Byl G, Catania VD, Calisti A, Miele V (2015) Ultrasound in newborns and children suffering from nontraumatic acute abdominal pain: imaging with clinical and surgical correlation. J Ultrasound 18:385–393. doi:10.1007/s40477-014-0087-4. Epub 2014 Apr 9
Dietrich RB, Kangarloo H, Lenarsky C, Feig SA (1987) Neuroblastoma: the role of MR imaging. AJR Am J Roentgenol 148:937–942
Dodd GD, Budzik RF (1990) Lipomatous tumors of the pelvis in women: spectrum of imaging findings. AJR Am J Roentgenol 155:317–322
Douglass EC, Reynolds M, Finegold M et al (1993) Cisplatin, vincristine, and fluorouracil therapy for hepatoblastoma: a Pediatric Oncology Group study. J Clin Oncol 11:96–99
Dresler S, Harvey DG, Levisohn PM (1979) Retroperitoneal neuroblastoma widely metastatic to the central nervous system. Ann Neurol 5:196–198
Evans AE, Siber JH, Shipilsky A et al (1996) Successful management of low stage neuroblastoma without adjuvant therapies: a comparison of two decades, 1972 through 1981 and 1982 through 1992, in a single institution. J Clin Oncol 14:2504–2510
Feusner JH, Ortega J, Haas J, Quinn J, King A, Ablin A et al (1997) Hepatoblastoma in premature infants. Proc Am Soc Clin Oncol 16:525a
Fishman EK, Harman DS, Goldman SM et al (1983) The CT appearance of Wilms' tumor. J Comput Assist Tomogr 7:659–665
Fragkandrea I, Nixon JA, Panagopoulou P (2013) Signs and symptoms of childhood cancer: a guide for early recognition. Am Fam Physician 88:185–192
Frappaz D, Giammarile F, Thiesse P et al (1997) False positive MIBG scan. Med Pediatr Oncol 29:589–592
Ganguly A, Gribble J, Tune B et al (1973) Renin-secreting Wilms' tumor with severe hypertension: report of a case and brief review of renin-secreting tumors. Ann Intern Med 79:835–837
Gilday DL, Ash JM, Reilly BJ (1977) Radionuclide skeletal survey for pediatric neoplasms. Radiology 123:399–406
Golden CB M.D., Feusner JH M.D. (2002) Malignant abdominal masses in children: quick guide to evaluation and diagnosis. Pediatr Clin N Am 49:1369–1392
Graham-Pole J, Salmi T, Anton AH et al (1983) Tumor and urine catecholamines (CATS) in neurogenic tumors. Correlations with other prognostic factors and survival. Cancer 51:834–839
Green DM (2008) Chemotherapy for the treatment of children and adolescents with malignant germ cells tumors (GCT). J Clin Oncol 20:3297–3298
Green DM, D'Angio GL, Beckwith JB et al (1996) Wilms' tumor. CA Cancer J Clin 46:46–63
Grundy P, Koufos A, Morgan K et al (1988) Familial predisposition to Wilms' tumor does not map to the short arm of chromosome 11. Nature 336:374–376
Guinet C, Buy JN, Ghossain MA et al (1993) Fat suppression technique in MR imaging of mature ovarian teratomas: comparison with CT. Eur J Radiol 17:117–121
Hattner RS, Huberty JP, Engelstad BL, Gooding CA, Ablin AR (1984) Localization of m-iodo(131I)-benzylguanidine in neuroblastoma. AJR Am J Roentgenol 143:373–374
Heisel MA, Miller JH, Reid BS, Siegel SE (1983) Radionuclide bone scan in neuroblastoma. Pediatrics 71:206–209
Imaoka I, Sugimura K, Okizuka H et al (1993) Ovarian cystic teratomas: value of chemical fat saturation magnetic resonance imaging. Br J Radiol 66:994–997
Joshi VV, Cantor AB, Altshuler G et al (1992) Age-linked prognostic categorization based on a new histologic grading system of neuroblastomas: a clinopathologic study of 211 cases from the Pediatric Oncology Group. Cancer 69:2197–2211
Kammer BF, Matthay KK, Pacharn P et al (2001) Pulmonary metastases at diagnosis of neuroblastoma in pediatric patients: CT findings and prognosis. AJR Am J Roentgenol 176:755–759
Kenny BJ, Pizer BL, Duncan AW, Foreman NK (1995) Cystic cerebral neuroblastoma. Pediatr Radiol 25(suppl 1): S97–S98
Keslar PJ, Buck JL, Suarez ES (1994) Germ cell tumors of the sacrococcygeal region: radiologic pathologic correlation. Radiographics 14:607–620
Kimura I, Togashi K et al (1994) Ovarian torsion: CT and MRI imaging appearances. Radiology 190: 337–341
King D, Goodman J, Hawk T, Boles ET, Sayers MP (1975) Dumbbell neuroblastomas in children. Arch Surg 110:888–891
Kingston JE, Herbert A, Draper GJ et al (1983) Association between hepatoblastoma and polyposis coli. Arch Dis Child 58:959–962
Kinnier-Wilson LM, Draper GJ (1974) Neuroblastoma, its natural history and prognosis: a study of 487 cases. BMJ 3:301–307
Kramer K, Kushner B, Heller G et al (2001) Neuroblastoma metastatic to the central nervous system. Cancer 91:1510–1519
Kushner BH, Cheung NK, LaQuaglia P et al (1996) Survival from locally invasive or widespread neuroblastoma without cytotoxic therapy. J Clin Oncol 14:373–381
Laug WE, Siegel SE, Shaw KNF et al (1978) Initial urinary catecholamine metabolite concentrations and prognosis in neuroblastoma. Pediatrics 62:77–83
Li FP, Thurber WA, Seddon J et al (1987) Hepatoblastoma in families with polyposis coli. JAMA 257:2475–2477
Lonergan GJ, Martinez-Leon MI, Agrons GA, Montemarano H, Suarez ES (1998) Nephrogenic rests,

nephroblastomatosis, and associated lesions of the kidney. RadioGraphics 18:947–968
Malkasian GD, Symmonds GD, Dockerty MB (1965) Malignant ovarian teratomas. Obstet Gynecol 25: 810–814
Marsden HB, Lawler W (1983) Primary renal tumors in the first year of life. A population-based review. Virchows Arch A Pathol Anat Histopathol 399:1–9
Marten DF, Kirks DR (1985) Diagnostic imaging of pediatric abdominal masses. Pediatr Clin North Am 32: 1397–1425
Matthay KK (1995) Neuroblastoma: a clinical challenge and biologic puzzle. CA Cancer J Clin 45:179–192
Matthay KK, Sather HN, Seeger RC et al (1989) Excellent outcome of stage II neuroblastoma is independent of residual disease and radiation therapy. J Clin Oncol 7:236–244
Matthay KK, Lukens J et al (1994) Outcome and prognostic factors for 1008 children with neuroblastoma treated from 1989–1995 on Children's Cancer Group (CCG) protocols. 6th symposium on Advances in Neuroblastoma Research. Philadelphia, PA, May 13–15, 1993. Prog Clin Biol Res 385:1–448
Matz MH (1961) Benign cystic teratomas of the ovary. Obstet Gynecol Surv 16:591–605
Maurer HM, Beltangady M, Gehan EA et al (1988) The intergroup rhabdomyosarcoma study I: a final report. Cancer 61:209–220
Menichini G, Sessa B, Trinci M, Galluzzo M, Miele V (2015) Accuracy of contrast-enhanced ultrasound in the identification and characterization of traumatic solid organ lesions in children: a retrospective comparison with baseline-US and CE-MDCT. Radiol Med 120:989–1001
Miele V, Di Giampietro I (2014) Diagnostic Imaging in Emergency. Salute e Società, (2EN):127–138. doi: 10.3280/SES2014-002010EN
Miele V, Morucci M, Bibbolino C, Calisti A, De Medici L, Valenti M (1996) Imaging diagnosis in a case of adrenal cystic ganglioneuroblastoma in a child. Radiol Med 91:485–458
Miele V, Galluzzo M, Bellussi A, Valenti M (1998a) Spiral computerized tomography in the study of renal neoplasms in children. Radiol Med 95:486–492
Miele V, Galluzzo M, Cortese A, Patti G, Bellussi A (1998b) Spiral CT study in a case of multifocal hepatoblastoma with atypical features. Radiol Med 95:386–388
Miele V, Stasolla A, Sergi D, Adami L, Calisti A (1999) A neonatal sacrococcygeal teratoma studied by spiral computed tomography. A case report. Radiol Med 98:401–403
Miele V, Andreoli C, Cortese A, De Cicco ML, Luzietti M, Stasolla A, David V (2002) Hemoperitoneum following ovarian cyst rupture: CT usefulness in the diagnosis. Radiol Med 104:122–126
Miele V, Andreoli C, Grassi R (2006) The management of emergency radiology: key facts. Eur J Radiol 59:311–314
Miele V, Di Giampietro I, Ianniello S, Pinto F, Trinci M (2015) Diagnostic imaging in pediatric polytrauma management. Radiol Med 120:33–49
Miele V, Piccolo CL, Sessa B, Trinci M, Galluzzo M (2016a) Comparison between MRI and CEUS in the follow-up of patients with blunt abdominal trauma managed conservatively. Radiol Med 121:27–37
Miele V, Piccolo CL, Galluzzo M, Ianniello S, Sessa B, Trinci M (2016b) Contrast enhanced ultrasound (CEUS) in blunt abdominal trauma. Br J Radiol 89(1061):20150823. doi:10.1259/bjr.20150823Epub2016Jan8
Miele V, Piccolo CL, Trinci M, Galluzzo M, Ianniello S, Brunese L (2016c) Diagnostic imaging of blunt abdominal trauma in pediatric patients. Radiol Med 121:409–430. doi:10.1007/s11547-016-0637-2. Epub 2016 Apr 13
Morris JA, Shcochat SJ, Smith EI et al (1995) Biological variables in thoracic neuroblastoma: a pediatric oncology group study. J Pediatr Surg 30:296–302, discussion: 302-303
Nitschke R, Smith EI, Shochat S et al (1988) Localized neuroblastoma treated by surgery: a Pediatric Oncology Group study. J Clin Oncol 6:1271–1279
Occhipinti KA, Frankel SD, Hricak H (1993) The ovary: computed tomography and magnetic resonance imaging. Radiol Clin North Am 31:1115–1132
Outwater EK, Dunton CJ (1995) Imaging of the ovary and adnexa: clinical issues and applications of MR imaging. Radiology 194:1–18
Pantoja E, Llobet R, Gonzalez-Flores B (1976) Retroperitoneal teratoma: histological review. J Urol 115:520–523
Patel MD, Feldstein VA, Lipson SD et al (1998) Cystic teratomas of the ovary: diagnostic value of sonography. AJR Am J Roentgenol 171:1061–1065
Perez CA, Matthay KK et al (2000) Biologic variables in the outcome of stages I and II neuroblastoma treated with surgery as primary therapy: a Children's Cancer Group study. J Clin Oncol 18:18–26
Pinto E, Guinard JP (1995) Renal masses in the neonate. Biol Neonate 68:175–184
Pinto F, Miele V, Scaglione M, Pinto A (2014) The use of contrast-enhanced ultrasound in blunt abdominal trauma: advantages and limitations. Acta Radiol 55:776–784
Pinto F, Valentino M, Romanini L, Basilico R, Miele V (2015) The role of CEUS in the assessment haemodynamically stable patients with blunt abdominal trauma. Radiol Med 120:3–11
Quinn SF, Erickson S, Black WC (1985) Cystic ovarian teratomas: the sonographic appearance of the dermoid plug. Radiology 155:477–478
Rescorla FJ (2008) Malignant germ cell tumors. In: Carachi R, Grosfeld JL, Azmy AF (eds) The surgery of childhood tumors, 2nd edn. Springer –Verlag, Heidelberg, pp 261–273
Rescorla FJ (2012) Pediatric germ cell tumors. Semin Pediatr Surg 21:51–60

Riccabona M (2003) Imaging of renal tumours in infancy and childhood. Eur Radiol 13(Suppl 4):L116–L129

Roos JE, Pfiffner R, Stallmacj T et al (2003) Infantile hemangioendothelioma. Radiographics 23:1649–1655

Schnater JM, Kohler SE, Lamers WH et al (2003) Where do we stand with hepatoblastoma? A review. Cancer 98:668–678

Seeger RC, Brodeur GM, Sather H et al (1985) Association of multiple copies of the N-myc oncogene with rapid progression of neuroblastomas. N Engl J Med 313:1111–1116

Selby DM, Stocker JT, Waclawiw MA et al (1994) Infantile hemangioendothelioma of the liver. Hepatology 20:39–45

Sessa B, Trinci M, Ianniello S, Menichini G, Galluzzo M, Miele V (2015) Blunt abdominal trauma: role of contrast-enhanced ultrasound in the detection and staging of abdominal traumatic lesions compared with US and CE-MDCT. Radiol Med 120: 180–189

Shalaby-Rana E, Majd M, Andrich MP, Movassaghi N (1997) In-111 pentetreotide scintigraphy in patients with neuroblastoma: comparison with I-131 MIBG, Nmyc oncogene amplification, and patient outcome. Clin Nucl Med 22:315–319

Shimada H, Ambros IM, Dehner LP (1999) The international neuroblastoma pathology classification (the Shimada system). Cancer 86:364–372

Shulkin BL, Shapiro B, Hutchinson RJ (1992) Iodine-131-metaiodobenzylguanidine and bone scintigraphy for the detection of neuroblastoma. J Nucl Med 33:1735–1740

Siegel MJ, Jamroz GA, Glazer HS, Abramson CL (1986) MR imaging of intraspinal extension of neuroblastoma. J Comput Assist Tomogr 10:593–595

Stark DD, Moss AA, Brasch RC et al (1983) Neuroblastoma: diagnostic imaging and staging. Radiology 148:101–105

Sutton CL, McKinney CD et al (1992) Ovarian masses revisited: radiologic and pathologic correlation. Radiographics 12:853–877

Talerman A (1994) Germ cell tumors of the ovary. In: Kurman RJ (ed) Blaustein's pathology of the female genital tract, 4th edn. Springer, New York, pp 849–914

Templeman CL, Fallat ME (2005) Benign ovarian masses. Semin Pediatr Surg 14:93–99

Togashi K, Nisghimura K, Itoh K et al (1987) Ovarian cystic teratomas: MR imaging. Radiology 162:669–673

Von Allmend D (2005) Malignant lesions of the ovary in childhood. Semin Pediatr Surg 14:100–105

White KS, Grossman H (1991) Wilms' and associated renal tumors of childhood. Pediatr Radiol 21:81–88